

**NUMERICAL MODEL FOR STEEL CATENARY RISER
ON SEAFLOOR SUPPORT**

A Thesis

by

JUNG HWAN YOU

Submitted to the Office of Graduate Studies of
Texas A&M University
in partial fulfillment of the requirements for the degree of
MASTER OF SCIENCE

December 2005

Major Subject: Civil Engineering

**NUMERICAL MODEL FOR STEEL CATENARY RISER
ON SEAFLOOR SUPPORT**

A Thesis

by

JUNG HWAN YOU

Submitted to the Office of Graduate Studies of
Texas A&M University
in partial fulfillment of the requirements for the degree of
MASTER OF SCIENCE

Approved by:

Chair of Committee,	Charles Aubeny
Committee Members,	Don Murff
	Giovanna Biscontin
	Jerome J. Schubert
Head of Department,	David V. Rosowsky

December 2005

Major Subject: Civil Engineering

ABSTRACT

Numerical Model for Steel Catenary Riser
on Seafloor Support. (December 2005)

Jung Hwan You, B.S., Yeungnam University

Chair of Advisory Committee: Dr. Charles Aubeny

Realistic predictions of service life of steel catenary risers (SCR) require an accurate characterization of seafloor stiffness in the region where the riser contacts the seafloor, the so-called touchdown zone. This thesis presents the initial stage of development of a simplified seafloor support model. This model simulates the seafloor-pipe interaction as a flexible pipe supported on a bed of springs. Constants for the soil springs were derived from finite element studies performed in a separate, parallel investigation. These supports are comprised of elasto-plastic springs with spring constants being a function of soil stiffness and strength, and the geometry of the trench within the touchdown zone.

Deflections and bending stresses in the pipe are computed based on a finite element method and a finite difference formulation developed in this research project. The finite difference algorithm has capabilities for analyzing linear springs, non-linear springs, and springs having a tension cut-off. The latter feature simulates the effect of a pipe pulling out of contact with the soil.

The model is used to perform parametric studies to assess the effects of soil

stiffness, soil strength, trench geometry, amplitude of pipe displacements, pipe stiffness, and length of touchdown zone on pipe deflections and bending stresses.

In conclusions, the seafloor stiffness (as characterized by the three spring parameters), the magnitude of pipe displacement, and the length of the touchdown zone all influence bending stresses in the pipe. Also, the tension cutoff effect, i.e., the pipe pulling away from the soil, can have a very large effect on bending stresses in the pipe. Neglecting this effect can lead to serious over-estimate of stress levels and excessive conservatism in design.

DEDICATION

To my family and my wife, Su Jung Park.

ACKNOWLEDGEMENTS

I would like to express my appreciation to all those who gave me the possibility to complete this thesis. Most of all, I would like to express my deep and sincere gratitude to my advisor, Dr. Charles Aubeny. His encouragement, time, and personal guidance helped me complete this thesis. I appreciate my committee members, Dr. Don Murff, Dr. Giovanna Biscontin and Dr. Jerome Schubert, for their advice and encouragement.

I would like to express my thanks to all my friends, and special thanks to Partha and Hansi, for helping me on this research. I would also like to thank Chun Ho Park for his encouragement.

I owe lots of love to my family. I deeply appreciate my parents for their endless support and encouragement in my life. I would also like to thank my two sisters. Last of all, I would like to express my appreciation to my lovely wife, Su Jung Park and her family. Her dedication and encouragement led me to the completion of this thesis.

TABLE OF CONTENTS

	Page
ABSTRACT	iii
DEDICATION	v
ACKNOWLEDGEMENTS	vi
TABLE OF CONTENTS	vii
LIST OF FIGURES	ix
LIST OF TABLES	xiii
 CHAPTER	
I INTRODUCTION	1
1.1. General	1
1.1.1 Steel Catenary Riser (SCR).....	2
1.1.2 Touchdown Point (TDP).....	3
1.2. Objective of Work	3
1.3. Thesis Contents	4
II BACKGROUND.....	5
2.1 Literature Review.....	6
2.2 Finite Difference Method.....	16
III NUMERICAL MODELING	19
3.1. Introduction.....	19
3.2. Finite Element Analysis.....	21
3.2.1. ABAQUS Formulation.....	21
3.2.2. FEM Results.....	28
3.3. Finite Difference Analysis.....	33
3.3.1. Construction of FD Model.....	33
3.3.2. FD Model with Linear Spring.....	40
3.3.3. FD Model with Nonlinear Spring.....	41
3.3.4. FD Model with Tension Cut-off Spring.....	42
3.3.5. FD Model Results.....	43

TABLE OF CONTENTS (Continued)

CHAPTER	Page
IV PARAMETRIC STUDIES	45
4.1. Introduction.....	45
4.2. Load-Deformation(P- δ) Curve Characteristics.....	46
4.3. Soil to Pipe Stiffness.....	52
4.4. Amplitude of Steel Catenary Riser Motions.....	57
V SUMMARY, CONCLUSIONS, AND RECOMMENDATIONS.....	60
5.1. Summary and Conclusions	60
5.2. Recommendation for Future Research	62
REFERENCES.....	64
APPENDIX A	66
APPENDIX B	74
APPENDIX C	76
APPENDIX D	79
APPENDIX E	83
VITA	87

LIST OF FIGURES

FIGURE	Page
1.1 General Catenary Arrangement (Bridge et al., 2003)	2
2.1 Soil Suction Model (Bridge and Willis, 2002).....	8
2.2 Comparison of Test Data and Analytical Bending Moment Envelope (Bridge and Willis, 2002).....	10
2.3 Concept of Backbone & Load-Deformation Curves (Thethi and Moros, 2001).....	11
2.4 Illustration of Pipe/Soil Interaction (Bridge et al., 2004).....	13
2.5 Re-penetration Pipe/Soil Interaction Curves (Bridge et al., 2004)	14
2.6 Beam Resting on an Elastic Foundation.	16
3.1 Conceptual Sketch of Touchdown Zone.....	20
3.2 Simplified Spring Support Model.	20
3.3 Trench Configuration.	20
3.4 The simplified two-dimensional model.....	22
3.5 Effect of Mesh Refinement on the Maximum Bending Stress in Riser Pipe.	22
3.6 Default Integration of Pipe Section in a Plane. (ABAQUS manual, 2004)	24
3.7 SPRING1 Element (ABAQUS manual, 2004)	24

LIST OF FIGURES (Continued)

FIGURE	Page
3.8 Nonlinear Spring Force and Relative Displacement Relationship. (ABAQUS manual, 2004).....	24
3.9 Capped Normalized P- δ Curve.....	26
3.10 Boundary Conditions of the Model.....	27
3.11 Bending Stress Variation for Nodal Densities.	29
3.12 Deflection Variation for Nodal Densities.....	29
3.13 Bending Stress Variation for Diameter of Riser Pipe	30
3.14 Bending Stress Variation for Thickness of Riser Pipe.....	30
3.15 Bending Stress Variation for Amplitude of Load	31
3.16 Bending Stress Change for Spring Type.....	32
3.17 Node Numbering in the Pipe when the Number of Element is 200.....	33
3.18 Rectangular Beam Fixed Two Ends.....	36
3.19 Deflection Change along Pipe Length for Figure 3.18	37
3.20 Bending Moment Change along Pipe Length for Figure 3.18	37
3.21 Flow Chart of FD Model with Nonlinear Soil Spring.....	39
3.22 P- δ Curve of Linear Spring.	40
3.23 Comparison between FEA and FDA for Bending Stress along Pipe Length for Linear Spring	41
3.24 P- δ Curve of Nonlinear Spring.....	41

LIST OF FIGURES (Continued)

FIGURE	Page
3.25 Comparison between FEA and FDA for Bending Stress along Pipe Length for Nonlinear Spring.....	42
3.26 P- δ Curve of Tension Cut-off Spring.....	42
3.27 Bending Stress for Variable Types of Soil Spring.....	43
3.28 Deflection for Variable Types of Soil Spring.....	43
3.29 Bending Stress Variation for Influence of t_{co}	44
3.30 Deflection Variation for Influence of t_{co}	44
4.1 Pipe-Nonlinear Soil Spring Support Model.....	45
4.2 Effect of E_s/S_u on Elastic Stiffness ($H/D=0.5$).....	47
4.3 Deflection Change along Pipe Length for Various E_s/S_u ($H/D=1.0$, $u=1$ in).....	48
4.4 Bending Stress Change along Pipe Length for Various E_s/S_u ($H/D=1.0$, $u=1$ in).....	48
4.5 Effect of Trench Depth ($E_s/S_u =100$).....	49
4.6 Deflection Change along Pipe Length for Various H/D ($H/D=1.0$, $u=1$ in).....	50
4.7 Bending Stress Change along Pipe Length for Various H/D ($H/D=1.0$, $u=1$ in).....	50
4.8 Effect of Trench Width ($H/D=1.0$, $E_s/S_u=100$).....	51

LIST OF FIGURES (Continued)

FIGURE	Page
4.9 Effect of Ratio for Variable Ratio λ (W/D=1.0, u=1 in).....	54
4.10 Effect of Ratio E_s/S_u for Variable Ratio λ (H/D=1.0, u=1 in).....	54
4.11 Deflection Change along Pipe Length for Various S_u (H/D=1.0, $E_s/S_u=100$, u=1 in)	55
4.12 Bending Stress Change along Pipe Length for Various S_u (H/D=1.0, $E_s/S_u=100$, u=1 in)	56
4.13 Effect of Displacement of Pipe for Variable Ratio λ (W/D=1.0, $E_s/S_u=100$)	58
4.14 Deflection Change along Pipe Length for Various Displacement, u (W/D=1.0, $E_s/S_u=100$)	59
4.15 Bending Stress Change along Pipe Length of Pipe for Various Displacement,u (W/D=1.0, $E_s/S_u=100$)	59

LIST OF TABLES

TABLE	Page
2.1 Geotechnical Parameters of Clay Soil at Watchet Harbor (Bridge and Willis, 2002).....	7
3.1 Fixed Input Data for Figures in Section 3.2.2.	28
3.2 Input Data for Figures in Section 3.2.2.	28
3.3 Input Data for Figures in Section 3.3 ($E_s/S_u=100$, $H/D=1.0$, $W/D=1.0$)	40
4.1 Range of Ratio for H/D , E_s/S_u ($W/D=1.0$).....	46
4.2 A Range of k_0 (psi) Depend on the Ratio H/D and E_s/S_u ($S_u=1$ psi).....	52
4.3 A Range of λ Depend on the Ratio H/D and E_s/S_u ($S_u=1$ psi).....	53
4.4 A Range of δ_y (in) Depend on the Ratio H/D and E_s/S_u	57
4.5 A Range of u/δ_y Depend on the Ratio H/D and E_s/S_u	57

CHAPTER I

INTRODUCTION

1.1 GENERAL

Many systems have been developed in recent to exploit hydrocarbon resources in deep waters throughout the world. Lately, compliant systems composed of large floating structures tethered to the seafloor by mooring lines are selected rather than conventional gravity systems. The need for development of new designs for riser pipes transmitting petroleum product has been created by the appearance of these new systems. The steel catenary riser (SCR) is proving to commonly be the system of choice to meet this need. The advantage of this concept is that it allows reduced cost because the pipeline is extended to the vessel using standard grade steel. Additionally, the riser can be installed using the same lay vessel as the pipeline, saving a dedicated mobilization.

One of the major issues with SCR's is fatigue, which is strongly influenced by soil conditions in the touchdown zone (TDZ), the zone at which the catenary riser makes contact with the seabed. A potential fatigue failure is directly related to maximum bending stress and moment in the SCR, which depends on the stiffness and damping of the seafloor and the motions of the SCR. For example, an SCR on a soft seafloor will have reduced bending stresses when a load is applied, while the one on a rigid seafloor will have more critical bending stresses.

This thesis follows the style of *The Journal of Geotechnical and Geoenvironmental Engineering*.

1.1.1 Steel Catenary Riser (SCR)

The essential steel catenary concept is simple. A free hanging simple catenary riser is connected to a floating production vessel and the riser hangs at a prescribed top angle. It is free-hanging and smoothly extends down to the seabed at the touchdown point (TDP). At the TDP, the SCR buries itself in a trench and then gradually rises to the surface where it is effectively a static pipeline. SCR may be described as consisting of three sections as shown in Figure 1.1, below:

- Catenary zone, where the riser hangs in a catenary section
- Buried zone, where the riser is within a trench
- Surface zone, where the riser rests on the seabed

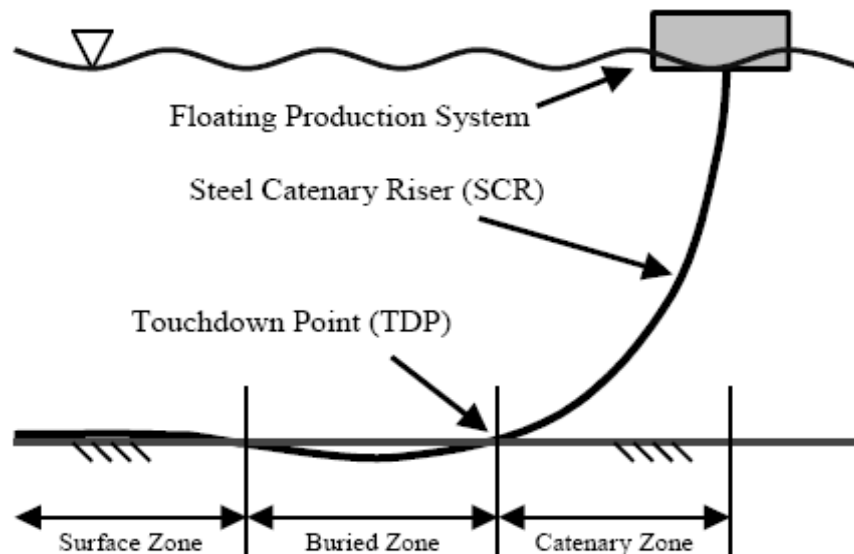


Figure 1. 1 General Catenary Arrangement (Bridge et al., 2003)

1.1.2 Touchdown Point (TDP)

The seabeds of deepwater oil and gas fields often consist of soft clay. In the buried zone beyond the TDP, deep trenches cut into the seabed. The mechanisms of trench formation are not well understood because the response of the riser at the seabed TDP and the interaction with the seabed is complex. However, it is thought that the dynamic motions of the riser, including scour, sediment transport, and seabed currents produce the trench. Also, storm and current action can pull the riser upwards from its trench, or laterally against the trench wall. Once a trench is formed there is a possibility that the trench may back-fill the trench and, over time, consolidate. Subsequent extreme vessel offsets may then result in higher stresses than those calculated on a rigid seabed, since the pipe must be sheared out of the soil and high suction forces must be overcome. This can concentrate curvature in the riser immediately above the TDP causing higher stresses, resulting in possible overstressing and a higher fatigue damage rate.

1.2 OBJECTIVE OF WORK

More detailed analysis of risers can be conducted using non-linear finite element analysis programs. Most riser analysis codes use either rigid or linear elastic contact surfaces to simulate the seabed, which model vertical soil resistance to pipe penetration, horizontal friction resistance and axial friction resistance (Bridge et al., 2003). Until recently most analysis was conducted assuming the seabed is rigid or that it exhibits a linear stiffness. A rigid surface generally gives a conservative result since it is unyielding, while the linear elastic surface is a better approximation of a seabed.

This thesis concentrates on conducting numerical studies to understand basic interaction mechanisms and on developing a simplified model for a seafloor interaction with steel catenary risers within the touchdown zone. The response of the seafloor to SCR movements will be studied to formulate a proper boundary condition at the seafloor touchdown zone for structural analysis of a riser subjected to vertical loading representing the vessel motion and seabed current. The relative importance of various seafloor and loading conditions on bending stresses of the riser pipe resting on nonlinear spring supports will also be investigated. This research concentrates on only vertical motions of riser pipe, although axial and lateral motions may have to be considered in the future.

1.3 THESIS CONTENTS

A brief description of the organization of the chapters that form this thesis follows:

Chapter II provides a summary of previous work reviewed for this investigation in the area of the steel catenary riser and basic concepts of the analysis such as the finite difference method.

Chapter III presents a finite element (FE) model and a finite difference (FD) model of SCR behavior for variable conditions of seafloor support and riser pipe properties.

Chapter IV presents parametric studies using developed FE model and FD model with nonlinear soil spring. The parametric studies include load-deformation ($P-\delta$)

curve characteristics, effect of soil and riser pipe stiffness, and amplitude of steel catenary riser motions.

Finally, Chapter V presents summary, conclusions, and recommendations for future research.

CHAPTER II

BACKGROUND

2.1 LITERATURE REVIEW

A number of studies have been directed toward understanding the mechanism of steel catenary riser behavior. The first, the full-scale test to research the effects of fluid, riser and soil interaction on catenary riser and stresses in riser pipe at the touch down point (TDP) was conducted over 3 months at Watchet Harbor in the west of England by the STRIDE III JIP, 2H Offshore Engineering Ltd in 2000 (Willis and West, 2001). The purpose of the full-scale test was to estimate the significance of fluid, riser and soil interaction and to develop finite element analysis techniques to predict the measured response.

A 110m (360ft) long 0.1683m (6-5/8inch) diameter riser pipe was used for this experiment. The riser was connected with an actuator on the harbor wall to an anchor point on the seabed. A programmable logic controller (PLC) to simulate the vessel drift and the wave motions of a platform in 1000m (3,300ft) water depth was used to actuate the top of the pipe string. Tensions and bending moments were monitored by installing strain gauges along the pipe length.

The seabed is made up of soft clay with an undrained shear strength of 3 to 5 kPa, a sensitivity of 3, a plasticity index of 39% and a normally consolidated shear strength gradient below the mud layer. Table 2.1 shows the geotechnical parameters for seabed soil in detail.

Table 2. 1 Geotechnical Parameters of Clay Soil at Watchet Harbor (Bridge and Willis, 2002)

Geotechnical Parameter	Value
Moisture Content, w	104.7%
Bulk Density, ρ	1.46 Mg/m ³
Dry Density, ρ_d	0.73 Mg/m ³
Particle Density, ρ_s	2.68 Mg/m ³
Liquid Limit, w_L	87.6%
Plastic Limit, w_P	38.8%
Plasticity Index, I_p	48.9%
Average Organic Content	3.2%
Specific Gravity, G_s	2.68
Undisturbed Shear Strength at 1D	3.5 kPa
Remoulded Shear Strength at 1D	1.7 kPa
Sensitivity of Clay at 1D	3.3
Coefficient of Consolidation, c_v at 1D	0.5 m ² /year
Coefficient of Volume Compressibility, m_v at 1D	15 m ² /MN

Bridge et al. (2003) reviewed the results of full-scale riser test by 2H Offshore Engineering Ltd. The authors concluded that the soil suction force, repeated loading, pull up velocity and the length of the consolidation time can affect the fluid, riser and soil interaction from the test data. Also it stated the possible causes for mechanisms for the trench creation as follows:

- The up and down motions of the pipe driven by actuator can form the trench. Also, water rushing out from beneath the riser can scour out a trench.
- Scouring and washing away of the sediment around the riser may be caused by the flow of the tides.

- The vortex induced vibration (VIV) motions which was observed when the tide came in or went out can result in the flow of the seawater across the riser. The high frequency motion would act such as a saw, slowly cutting into the seabed.
- The buoyancy force causes the riser to lift away from the seabed when the test riser is submerged. Any loose sediment in the trench or attached to the riser would be washed away.

Bridge and Willis (2002) conducted the analytical modeling to calibrate the soil suction model of 2H Offshore Engineering Ltd. The upper bound curve (Fig. 2.1) based on the STRIDE 2D pipe and soil interaction analysis (Wills and West, 2001) was employed as the soil suction curve in the analytical modeling. They stated that the soil suction curve consists of three parts which are suction mobilization, the suction plateau and suction release like Figure 2.1.

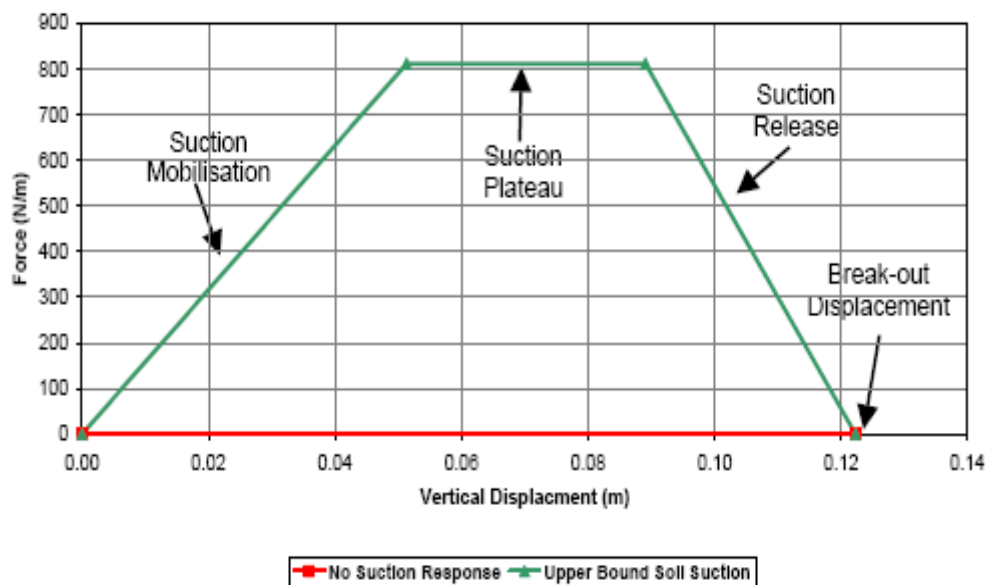


Figure 2. 1 Soil Suction Model (Bridge and Willis, 2002)

In addition, the each test measurement from a strain gauge location was compared to that of a similar point on the analytical model. Computed bending moments were bracketed by analytical predictions for with suction and no suction. The results of comparison showed good agreement as illustrated Figure 2.2. Further, they compared pull up and lay down response owing to the difference in bending moment between two response occurred by soil suction. The results of these comparisons are as follows:

- A sudden vertical displacement of a catenary riser at its touchdown point (TDP) after a period at rest could cause a peak in the bending stress.
- Soil suction forces are subject to hysteresis effects.
- The soil suction force is related to the consolidation time.
- Pull up velocity does not strongly correlate with the bending moment response on a remolded seabed.
- Soil suction can cause effects such as a suction kick.

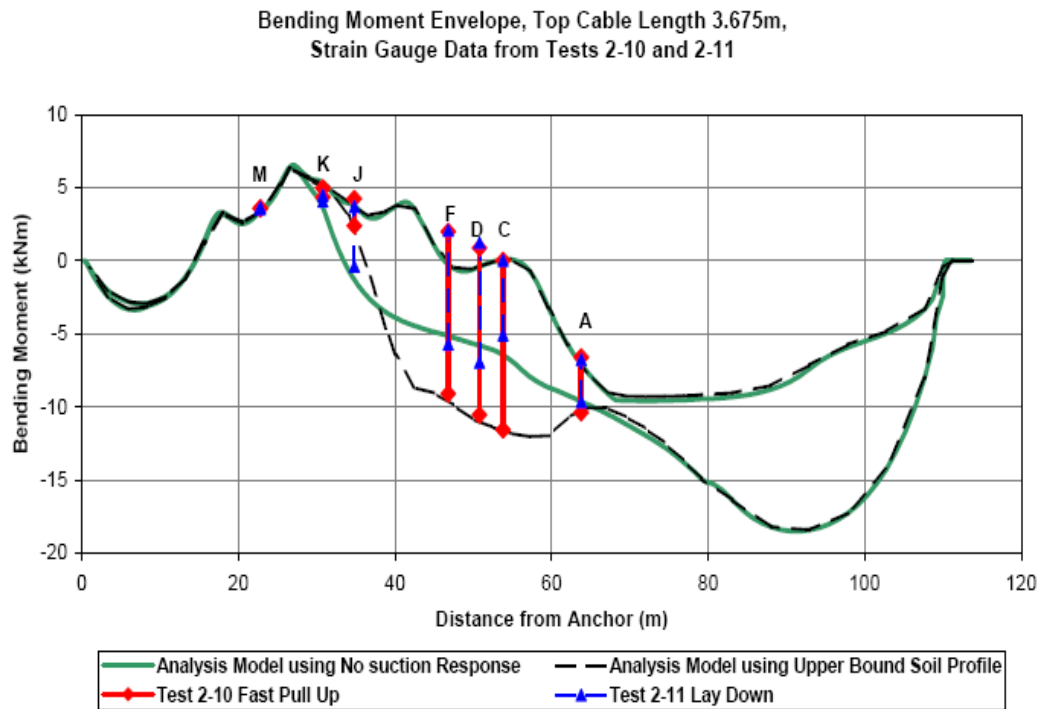


Figure 2. 2 Comparison of Test Data and Analytical Bending Moment Envelope (Bridge and Willis, 2002)

Thethi and Moros (2001) considered three aspects of soil-catenary riser interaction; the effect of riser motions on the seabed associated the vertical movement of the riser, the effect of water on the seabed related to pumping action, and the effect of the seabed on the riser related to vertical, lateral and axial soil resistance. Because of the complexity of the problem, Thethi and Moros recommend that trench depth and width profiles were selected in the riser analysis based on the deepest trenches and conservative soil strength assumptions.

Usually, riser-soil response curves can be described in terms of a soil spring. However, representing the soil response at a riser element by time-independent soil support spring is not possible due to time varying behavior related to the repeated

loading and plastic deformation of soils. Instead, the shape of the spring may change with time from a virgin curve of soil response to a degraded response. In addition, a riser element can have no contact over a large displacement range until the displacement becomes greater than previously experienced at which point the element may suddenly regain to contact with the virgin response curve. Riser and soil response curves may be considered as a load path bounded by the backbone curve. The concept is illustrated in Figure 2.3. The characteristics of this riser-seabed load deflection curve depend on the burial depth as well as the soil and riser properties.

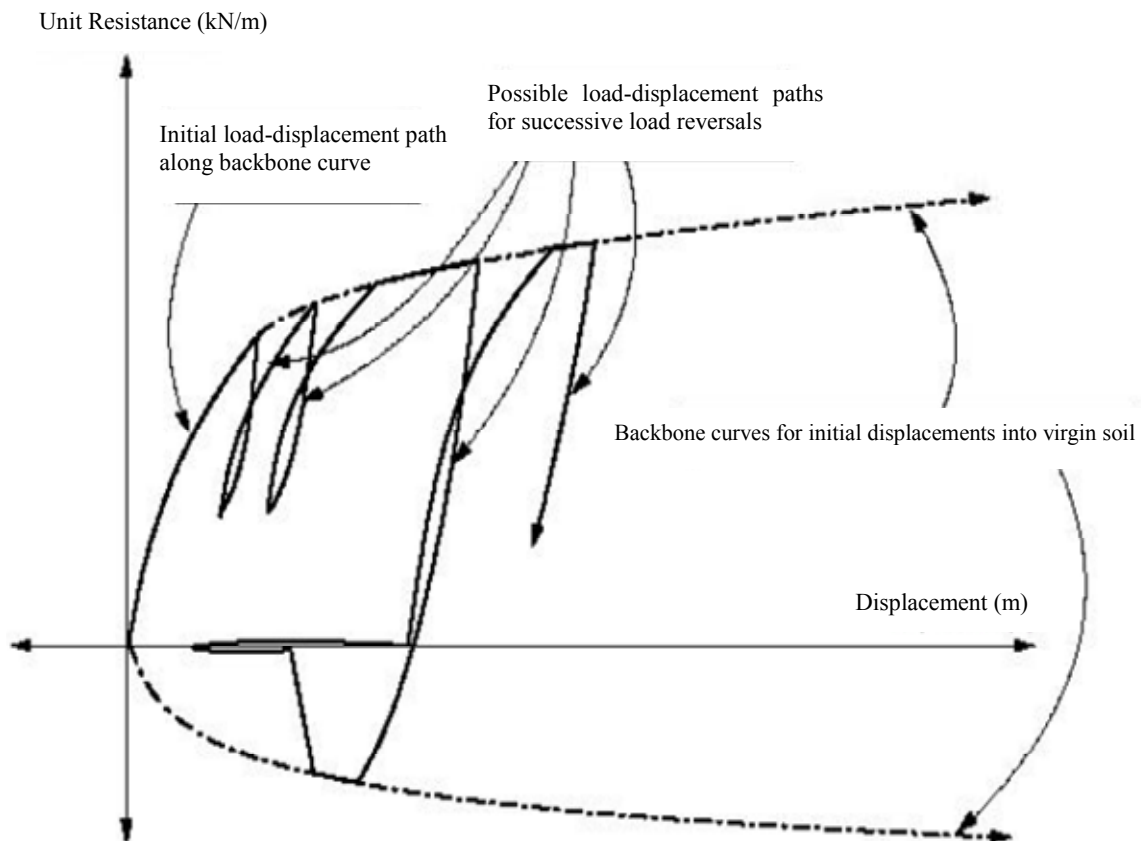


Figure 2. 3 Concept of Backbone & Load-Deformation Curves (Thethi and Moros, 2001)

Bridge et al. (2004) developed advanced models using published data and data from the pipe and soil interaction experiments conducted within the STRIDE and CARISIMA JIP's. They describe an example of the development of a pipe and soil interaction curve with an unloading and reloading cycle, as presented in Figure 2.4 and the mechanism of pipe and soil interaction such as following steps:

- (1) The pipe is initially in contact with a virgin soil.
- (2) The pipe penetrates into the soil, plastically deforming it. The pipe and soil interaction curve tracks on the backbone curve.
- (3) The pipe moves up and the soil acts elastically. The pipe and soil interaction curve move apart from the backbone curve, the force decreases over a small displacement.
- (4) The pipe resumes penetrating the soil, deforming it elastically. The pipe and soil interaction curve follows an elastic loading curve.
- (5) The pipe keeps going to penetrate into the soil, plastically deforming it. The pipe and soil interaction curve meets again with the backbone curve and tracks it.

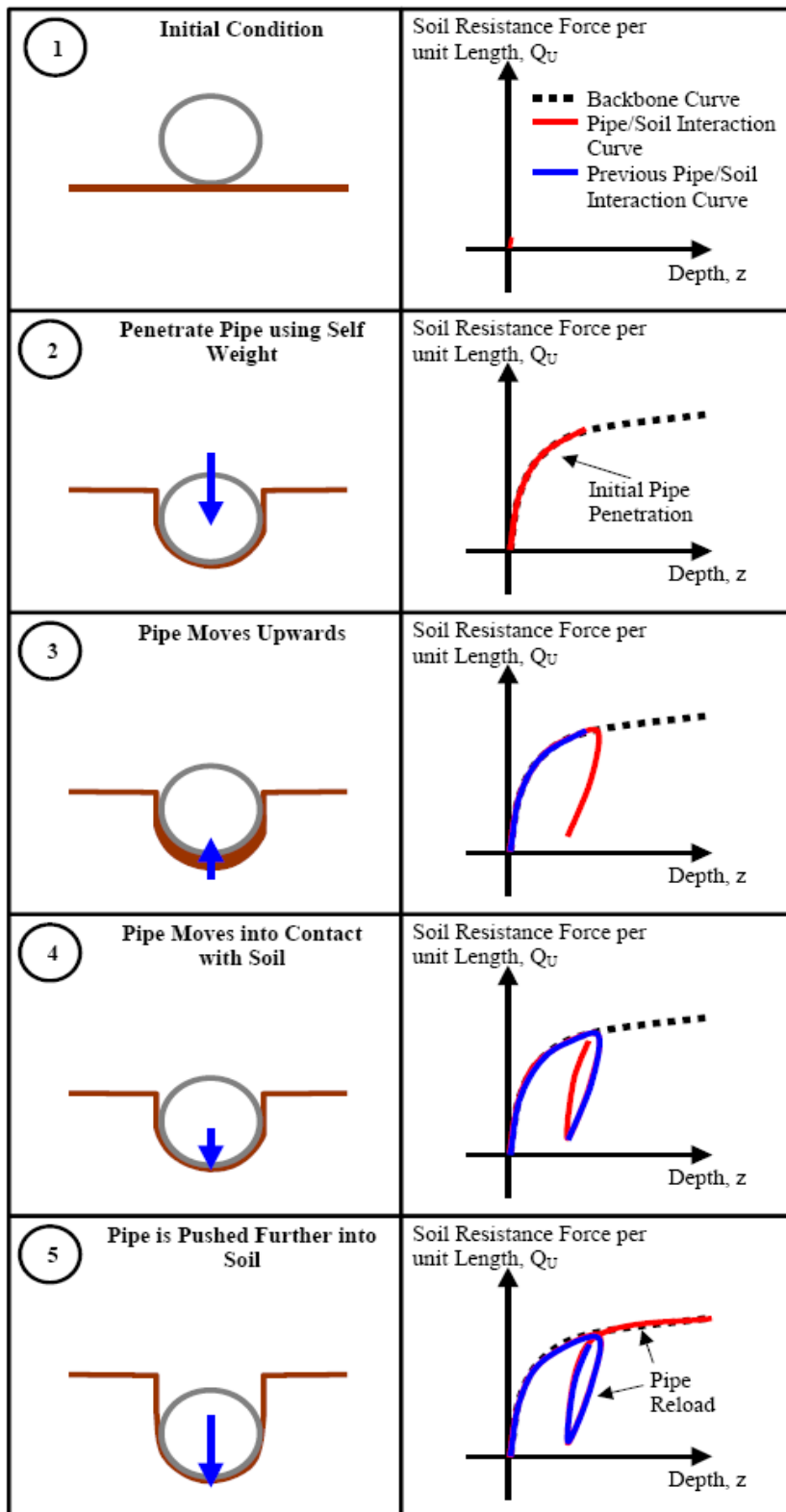


Figure 2. 4 Illustration of Pipe/Soil Interaction (Bridge et al., 2004)

In addition, they updated the force and displacement curve and consider the soil suction effect, as shown in Figure 2.5 and described below.

- (1) Penetration – the pipe penetrates into the soil to a depth where the soil force equals the penetration force.
- (2) Unloading – the penetration force reduces to zero allowing the soil to swell.
- (3) Soil suction – as the pipe continues to elevate the adhesion between the soil and the pipe causes a tensile force resisting the pipe motion. The adhesion force quickly increases to a maximum then decreases to zero as the pipe pulls out of the trench.
- (4) Re-penetration – the re-penetration force and displacement curve has zero force when the pipe enters the trench again, only increasing the interaction force when the pipe re-contacts the soil. The pipe and soil interaction force then increases until it rejoins the backbone curve at a lower depth than the previous penetration.

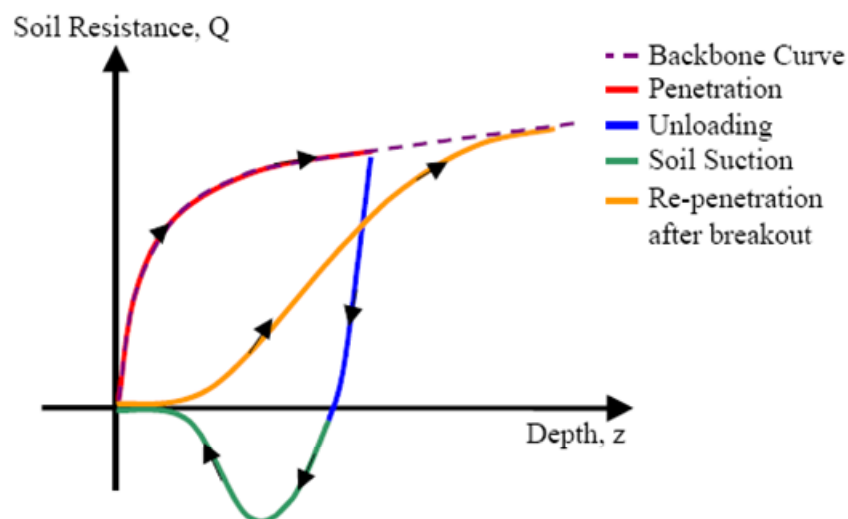


Figure 2. 5 Re-penetration Pipe/Soil Interaction Curves (Bridge et al., 2004)

C.P. Pesce, J.A.P. Aranha and C.A. Martins (1998) researched soil rigidity effect in the touch down boundary layer of riser on static problem. Their work developed previous analysis performed on the catenary riser TDP static boundary-layer problem by considering a linearly elastic soil. A non-dimensional soil rigidity parameter was defined as follows:

$$K = \frac{k\lambda^4}{EI} = \frac{k\lambda^2}{T_0} = \frac{kEI}{T_0^2} \quad (2.1)$$

Where k = the rigidity per unit area.

EI = the bending stiffness.

T_0 = the static tension at TDP

λ = the flexural-length parameter representing the TDP boundary later length scale.

A typical oscillatory behavior for the elasticity on the supported part of the pipe line was showed by the constructed solution. Also, it indicated how this behavior matched smoothly the catenary solution along the suspended part, removing the discontinuity in the shear effort, attained in the infinitely rigid soil case. In that previous case, the flexural length parameter $\lambda = \sqrt{EI/T_0}$ had been shown to be a measure for the position of the actual TDP, with regard to the ideal cable configuration.

Unlike the previous case, in the linearly elastic soil problem, the parameter λ has been shown to measure the displacement of the point of horizontal tangency about corresponding TDP attained in the ideal cable solution, in rigid soil. Having K as parameter some non-dimensional diagrams have been presented, showing, for $K \geq 10$, the

local elastic line, the horizontal angle, the shear effort, and the curvature, as functions of the local non-dimensional arc-length parameter $\varepsilon = s / \lambda$. Also, another non-dimensional curve was presented, enabling the determination of the actual TDP position as a function of soil rigidity K .

2.2 FINITE DIFFERENCE METHOD

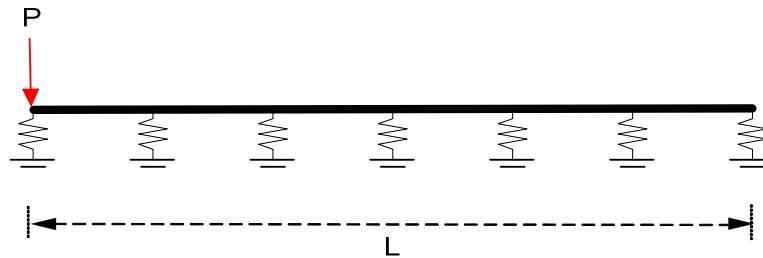


Figure 2. 6 Beam Resting on an Elastic Foundation

Assume a beam with bending stiffness EI rests on a foundation of elastic springs of stiffness k (Fig 2.6). The applied load is a concentrated load P acting on a location from the left end of the beam. Using standard method (Boresi and Schmidt, 2003) for calculating beam deflections:

$$q = -\frac{dV}{dx} \quad (2.2)$$

$$V = -\frac{dM}{dx} \quad (2.3)$$

$$M = EI \frac{d^2 y}{dx^2} \quad (2.4)$$

$$\frac{d^2}{dx^2} \left(EI \frac{d^2 y}{dx^2} \right) = q(x) \quad (2.5)$$

where q is the intensity of applied load and/or soil reaction, V is the internal shear force, M is the internal moment, E is the modulus of elasticity of pipe, I is the second moment of area of pipe, y is the deflection of the beam, and dx is the uniform size of elements into which the beam is subdivided.

For beams on elastic foundation and laterally loaded piles, the load intensity $q(x)$ is a function of lateral deflection y . For linear springs,

$$q(x) = -ky \quad (2.6)$$

where k is the spring constant of soil reaction which have a force per unit area. Also, each order differential equation can be expressed as follows:

$$\frac{dy}{dx} = \frac{y_{i+1} - y_{i-1}}{2(dx)} \sim \frac{y_i - y_{i-1}}{dx} \quad (2.7)$$

$$\frac{d^2 y}{dx^2} = \frac{1}{dx} \left[\frac{y_{i+1} - y_i}{dx} - \frac{y_i - y_{i-1}}{dx} \right] = \frac{y_{i+1} - 2y_i + y_{i-1}}{dx^2} \quad (2.8)$$

$$\frac{d^3 y}{dx^3} = \frac{1}{dx} \left[\frac{y_{i+2} - 2y_{i+1} + y_i}{dx^2} - \frac{y_{i+1} - 2y_i + y_{i-1}}{dx^2} \right] = \frac{y_{i+2} - 3y_{i+1} + 3y_i - y_{i-1}}{dx^3} \quad (2.9)$$

$$\frac{d^4 y}{dx^4} = \frac{1}{dx} \left[\frac{y_{i+2} - 3y_{i+1} + 3y_i - y_{i-1}}{dx^3} - \frac{y_{i+1} - 3y_i + 3y_{i-1} - y_{i-2}}{dx^3} \right] = \frac{y_{i+2} - 4y_{i+1} + 6y_i - 4y_{i-1} + y_{i-2}}{dx^4} \quad (2.10)$$

Finally, a finite difference form for a beam on elastic foundation (Desai and Christion, 1977) can be written

$$EI \left(\frac{y_{i-2} - 4y_{i-1} + 6y_i - 4y_{i+1} + y_{i+2}}{dx^4} \right) = -ky_i \quad (2.11)$$

Boundary conditions can be imposed as follows:

$$\text{Fixed displacement: } y_i = u_{imposed} \quad (2.12)$$

$$\text{Fixed slope: } \frac{dy}{dx} \approx \frac{y_i - y_{i-1}}{dx} \approx u'_{imposed} \quad (2.13)$$

$$\text{Fixed curvature: } \frac{d^2y}{dx^2} \approx \frac{y_{i+1} - 2y_i + y_{i-1}}{dx^2} \approx u''_{imposed} \quad (2.14)$$

For the case of a simple support, the displacement, $u_{imposed}$ and curvature (moment), $u''_{imposed}$ are set to zero. For the case of a fixed support, the displacement, $u_{imposed}$ and slope, $u'_{imposed}$ are set to zero.

CHAPTER III

NUMERICAL MODELING

3.1 INTRODUCTION

The actual SCR problem involves a pipe embedding itself into a soil continuum as shown in Figure 3.1. Rigorous analysis of this process would involve a full three-dimensional soil-structure interaction finite element analysis. This would involve intensive computational effort that is not justified at this early stage of the research. Therefore, an simplified approach is followed in this research.

The soil-pipe interaction is modeled as a pipe supported on springs as shown in Figure 3.2. Stiffness for the springs are obtained from 2D FEM analyses on soil-trench systems as illustrated in Figure 3.3, The FEM studies to calculate these spring constants are being determined in parallel study, separate from that presented in this thesis. The simplified model involves the following variables:

- Pipe properties: diameter of pipe (D), thickness of pipe (t),
modulus of elasticity of pipe (E_p)
- Soil properties: undrained shear strength of soil (S_u), modulus of soil (E_s)
- Geometry parameter: length of touch down zone (L),
pipe embedment (H), width of trench (W)
- Riser motion parameter: amplitude of riser movement (u)

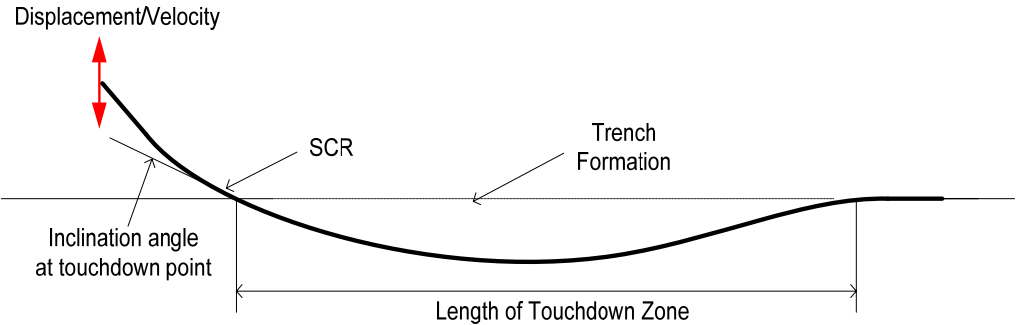


Figure 3. 1 Conceptual Sketch of Touchdown Zone

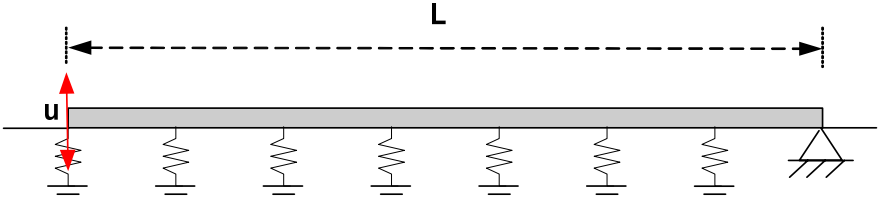


Figure 3. 2 Simplified Spring Support Model

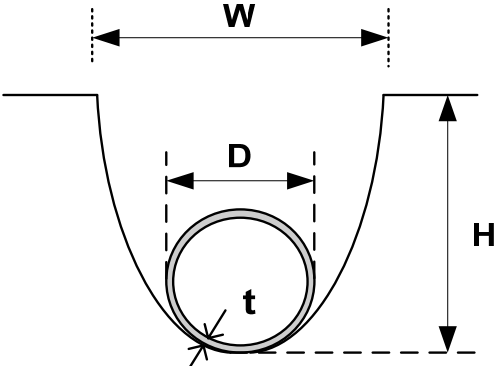


Figure 3. 3 Trench Configuration

3.2 FINITE ELEMENT ANALYSIS

FE analyses of SCR on seafloor support were conducted using the finite element code ABAQUS V6.4 (2003). ABAQUS is a versatile program which has been used in a lot of fields requiring FE analysis because it is capable of handling a wide range of problems and it shows considerably reliable results. In addition, this program was selected because of its easy accessibility on computers as well as its wide range of material and element modeling capabilities. The ABAQUS program requires grouped data such as node, element, boundary, material and loading to solve any FEM problem.

3.2.1 ABAQUS Formulation

Node

The code block for node defines the coordinates of all nodes in the used mesh with respect to a reference coordinate system. The simplified model with linear spring constant, k_0 is dx lb/in ($k_0 = [k_0]_{\text{norm}} * S_u * dx$, $[k_0]_{\text{norm}}$ is 1psi), which applied a displacement of 1in at the left end of the beam and hinged at the right end was simulated with the pipe and soil properties; length (L) is 300ft, diameter (D) is 6in, thickness (t) is 0.5in, modulus (E_p) of pipe is 30,000ksi, and undrained shear strength (S_u) is 1psi as shown in Figure 3.4. In addition, the number of nodes was increased from 10 nodes to 300 nodes to get a convergent maximum bending moment in the pipe riser from the model simulations. Figure 3.5 shows the result.

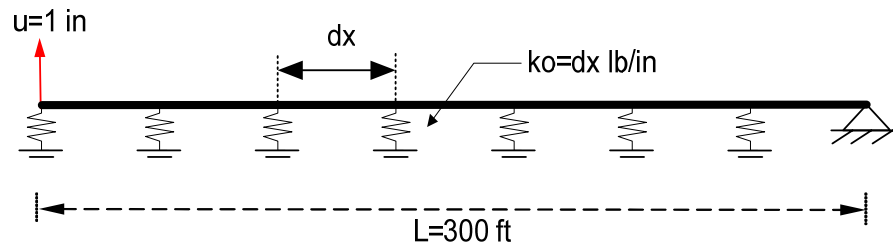


Figure 3. 4 The simplified two-dimensional model

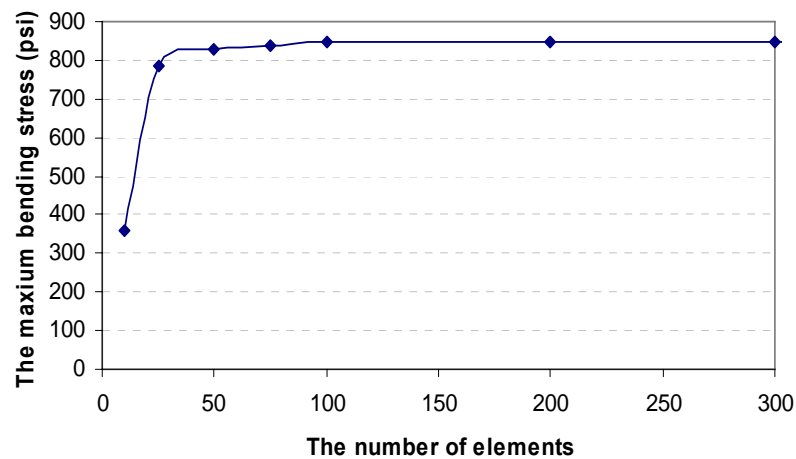


Figure 3. 5 Effect of Mesh Refinement on the Maximum Bending Stress in Riser Pipe

Element

A set of elements that act as a structural member are built by connecting the defined nodes. Basically, the simplified model consists of two different kinds of elements, a pipe element (PIPE21) which is a 2-dimensional, 2-node linear pipe and a spring element (SPRING1) which is the spring between a node and ground acting in a fixed direction. Each of the spring elements were connected to the all of pipe nodes except the last pipe node affected by boundary condition.

PIPE21 element is defined as a hollow, thin-walled, circular section beam

element obeying the beam theory in ABAQUS and it employs linear interpolation for displacements and constant interpolation for slope. Bending moments in this pipe section are always calculated about the centroid of the pipe section. The pipe axis is a line joining the nodes that define the beam element and it need not pass through the centroid of the beam section. Geometric input data such as outside radius (r) and wall thickness (t) of pipe is required to describe the pipe section. Figure 3.6 illustrates a pipe section which has five integration points by Simpson's rule.

The relative displacement across a SPRING1 element (Fig. 3.7) can be represented by the i th component of displacement of the spring's node:

$$\Delta u = u_i \quad (3.1)$$

where u_i is displacement in a vertical direction. The SPRING1 element can be linear or nonlinear. Linear spring behavior is defined by specifying constant spring stiffness, force per relative displacement (F/L), used as input data. However, when simulating the simplified FE model, the soil spring constant (F/L^2) obtained from the normalized load-deformation curve must be multiplied by the unit length (dx) of the pipe to get units of F/L . For nonlinear spring, a sufficiently wide range of force values and relative displacement values used as input data are provided in ascending order of relative displacement so that the behavior is defined correctly as shown in Figure 3.8.

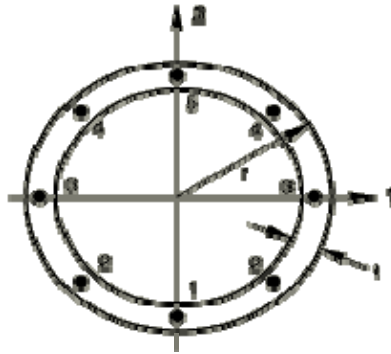


Figure 3. 6 Default Integration of Pipe Section in a Plane. (ABAQUS manual, 2004)



Figure 3. 7 SPRING1 Element (ABAQUS manual, 2004)

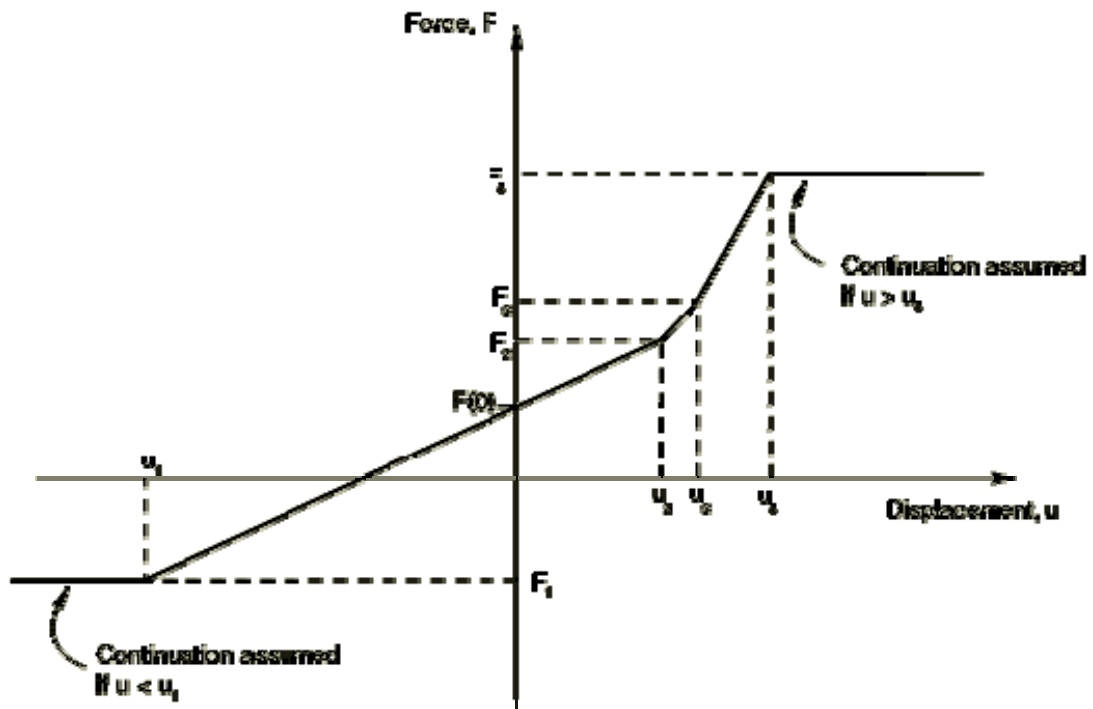


Figure 3. 8 Nonlinear Spring Force and Relative Displacement Relationship. (ABAQUS manual, 2004)

Material

Material models for all the materials were defined in this code block. Also, the elements were associated with corresponding material properties. This model consisted of two different kinds of materials, steel riser pipe and soil spring representing soil behavior. For steel riser pipe, a linear elastic model was used with an input variable, Young's modulus of pipe. For soil behavior, nonlinear spring that can yield was used with non-dimensional load-deformation (P- δ) curves.

A set of normalized load-deformation (P- δ) curves developed by Partha Sharma (personal communicator). He did a plane strain analysis with Elasto-Perfectly Plastic (EPP) model with Von Mises yield criteria to get the curves representing soil behavior. In addition, these curves considered some variables to see the effect of the trench geometry and ratio of elastic to plastic on the ultimate bearing capacity of the riser. The variables are the riser pipe embedment to the diameter of pipe (H/D ranging from 0.5 to 4.0), the trench width to the diameter of pipe (W/D ranging from 1.0 to 3.0) and the soil modulus to the undrained shear strength (E_s/S_u). E_s/S_u ranging from 100 to 1500 is employed as elastic parameter to see the effect on the force-displacement curve.

Also, The Normalized value of $\frac{P}{S_u D}$, where P is the ultimate load at failure, is used as plastic capacity.

The normalized nonlinear P- δ curves for soil spring were changed into simple bi-linear curves to characterize the springs in the simplified model as shown in Figure 3.9. For various material properties and geometric parameters, initial spring constant,

$(k_0)_{norm}$, as well as a maximum load, $(P_{max})_{norm}$, and a yield deformation, $(\delta_y)_{norm}$, are selected. For normalized loads below a certain $(P_{max})_{norm}$, the spring is linear and is described by a spring constant, $(k_0)_{norm}$. When the $(P_{max})_{norm}$ is reached, the spring resistance remains constant at $(P_{max})_{norm}$ and independent of the magnitude of deformation. In addition, the input data used in model can be obtained by the following calculation.

$$P_{max} [F] = (P_{max})_{norm} \cdot S_u \cdot D \cdot dx \quad (3.2)$$

$$k_0 [F/L] = (k_0)_{norm} \cdot S_u \cdot dx \quad (3.3)$$

$$\delta_y [L] = \frac{P_{max}}{k_0} = \frac{(P_{max})_{norm} \cdot S_u \cdot D}{(k_0)_{norm} \cdot S_u} = \left(\frac{P_{max}}{k_0} \right)_{norm} \cdot D \quad (3.4)$$

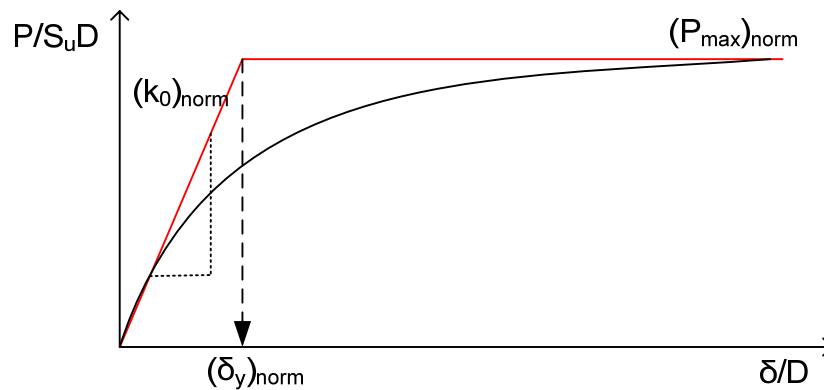


Figure 3. 9 Capped Normalized P- δ Curve

Boundary Conditions

A prescribed vertical displacement was imposed on the left-hand side, while the right-hand side was constrained vertically as shown in figure 3.10. In addition, all of spring nodes connected ground are fixed to vertical direction. This boundary condition can be formulated as

$$u_y = u \quad (\text{at } x = 0)$$

$$u_y = 0 \quad (\text{at } x = L)$$

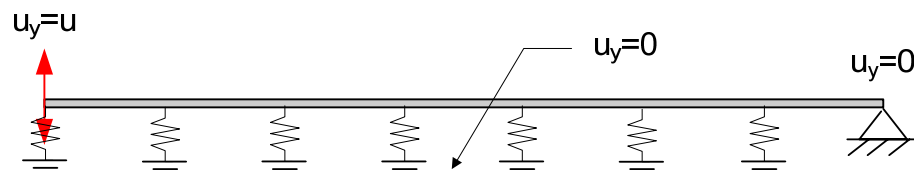


Figure 3. 10 Boundary Conditions of the Model

Loading

Load application is defined after establishing all the required conditions. In this simplified model, all kinds of loading which affect riser pipe are simply divided by two types of loading, upward and downward. These loadings are represented as displacements in the model, and also it is specified at the left end point in pipe.

3.2.2 FEM Results

All figures in this section result from FE model simulation with variable conditions as following Tables 3.1 and 3.2.

Table 3. 1 Fixed Input Data for Figures in Section 3.2.2

L	Ep	E/S _u	H/D	S _u	k _{norm}	(P _{max}) _{norm}	(δ _y) _{norm}
(ft)	(ksi)			(psi)	(psi)	(lb/in)	(in)
300	30,000	100	1.0	1.0	272	6.40	0.0235

Table 3. 2 Input Data for Figures in Section 3.2.2

Figure No.	3.11 & 3.12		3.13		3.14		3.15		3.16	
dx (in)	180	18	18	18	18	18	18	18	18	18
D (in)	6	6	6	12	6	6	6	6	6	6
t (in)	0.5	0.5	0.5	0.5	0.5	1.0	0.5	0.5	0.5	0.5
u (in)	6	6	6	6	6	6	6	12	6	6
spring type	linear	linear	nonlinear	nonlinear	nonlinear	nonlinear	nonlinear	nonlinear	linear	nonlinear
k ₀ (lb/in)	49015	4902	4902	4902	4902	4902	4902	4902	4902	4902
P _{max} (lbs)	6916	692	692	1383	692	692	692	692	692	692
δ _y (in)	0.141	0.141	0.141	0.282	0.141	0.141	0.141	0.141	0.141	0.141

Influence of Nodal Densities

Figure 3.11 illustrates the effect of mesh refinement. The maximum bending stress of fine mesh is higher than the one of coarse mesh for the same displacements. Also, fine mesh has the high curvature as showed Figure 3.12.

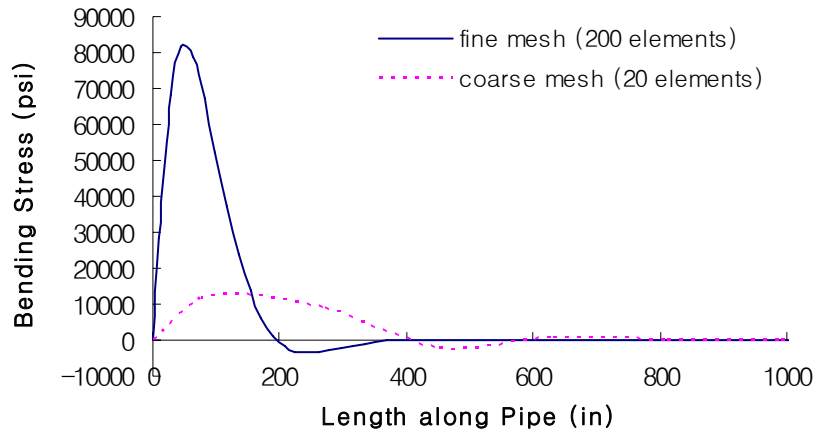


Figure 3. 11 Bending Stress Variation for Nodal Densities

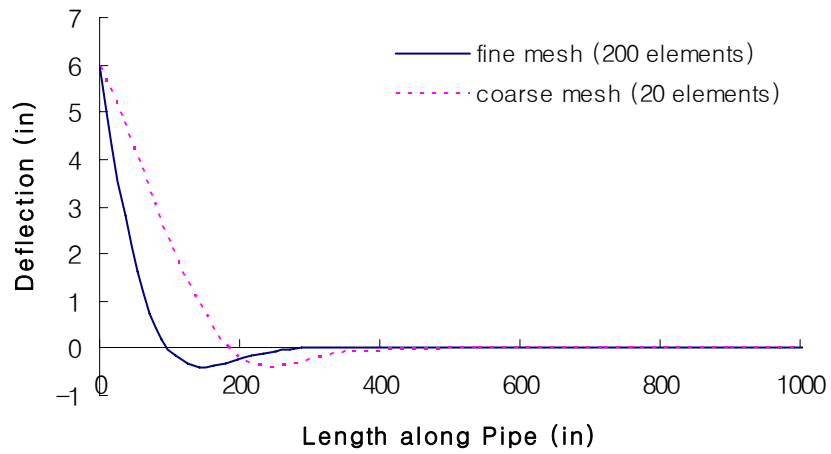


Figure 3. 12 Deflection Variation for Nodal Densities

Influence of Pipe Properties

The changes for different pipe properties such as diameter (D) and thickness (t) of pipe are showed in Figure 3.13 and 3.14. The more section area of pipe is small, the more bending stress in pipe is high as showed.

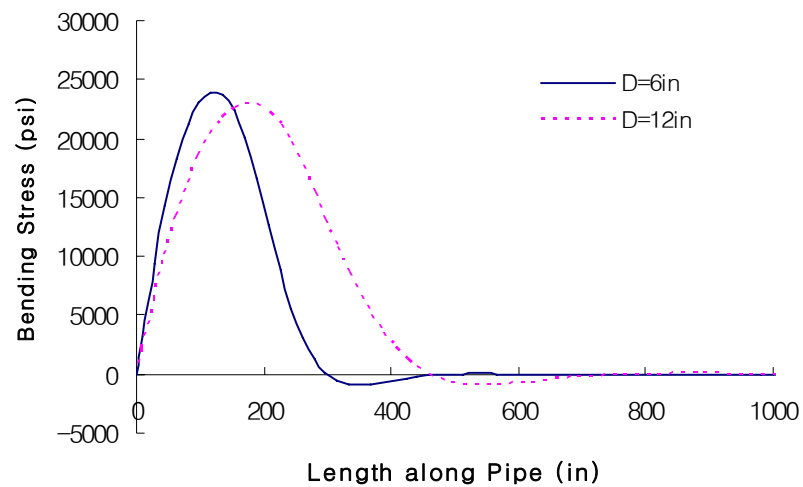


Figure 3. 13 Bending Stress Variation for Diameter of Riser Pipe

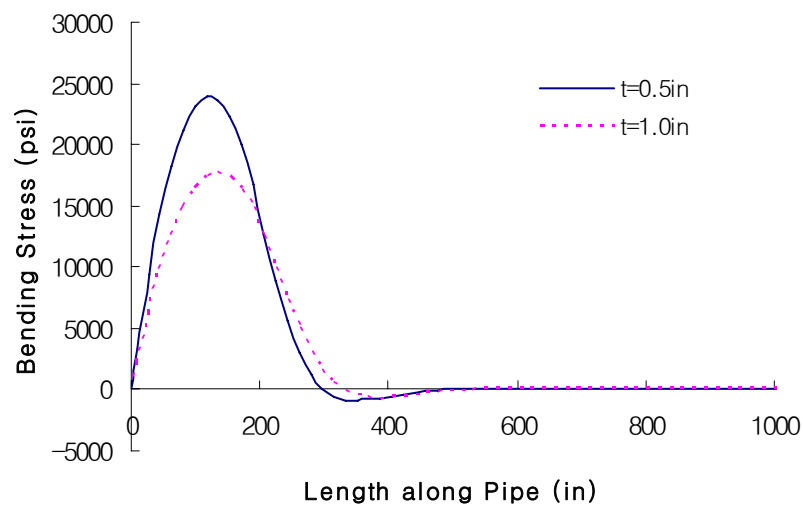


Figure 3. 14 Bending Stress Variation for Thickness of Riser Pipe

Influence of Amplitude of Load

Figure 3.15 illustrates effect for different sizes of load. The model is made by displacement control. Therefore, the displacement represents the load. The larger displacement makes higher bending stress.

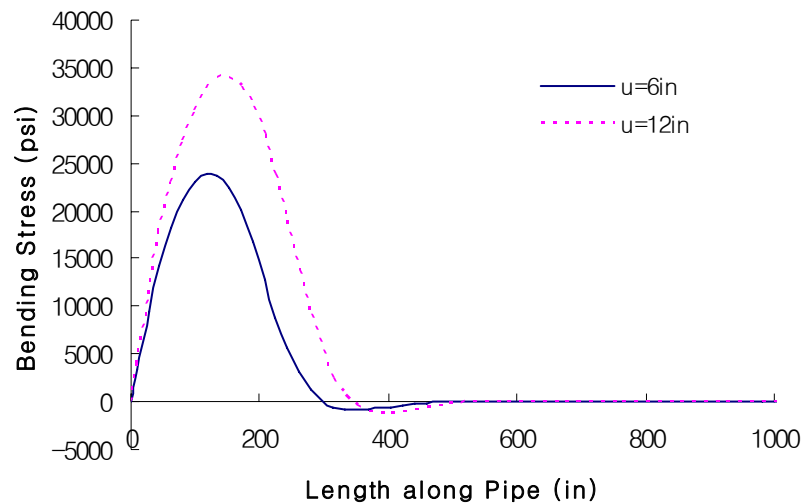


Figure 3. 15 Bending Stress Variation for Amplitude of Load

Influence of Spring Type

Figure 3.16 explains influence of spring type. For a linear spring model, the entire load is transmitted to the relative displacement in proportion to spring constant; however, nonlinear spring model can not reach the value over the maximum load and displacement. Therefore, the nonlinear spring model has lower bending stress.

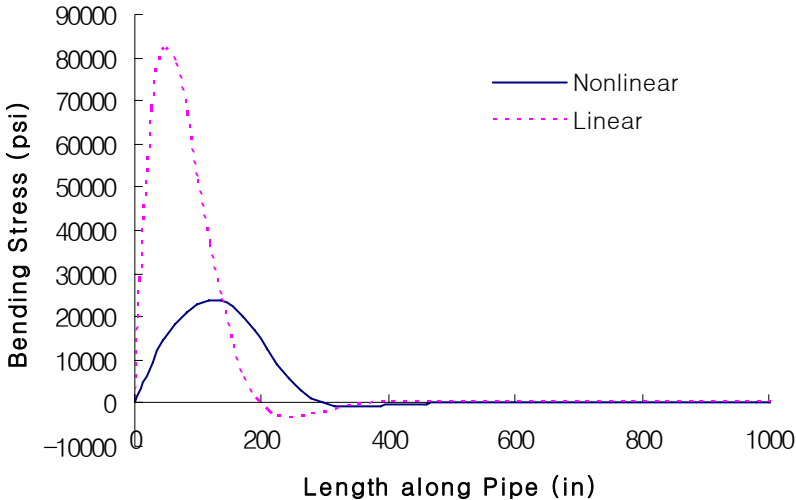


Figure 3. 16 Bending Stress Change for Spring Type

3.3 FINITE DIFFERENCE ANALYSIS

The starting point of FD studies is a one-dimensional finite difference analyses of a beam fixed at two ends without spring supports. In this FD simulation, uniformly distributed loads are applied along the pipe. The simulated result was compared with the analytical solution and the FE result to verify the accuracy of the FD model. Afterwards, the FD analyses are conducted in following order: pipe on the linear spring, pipe on the nonlinear spring having both compression and tension and pipe on the nonlinear tension cut-off spring.

3.3.1 Construction of FD Model

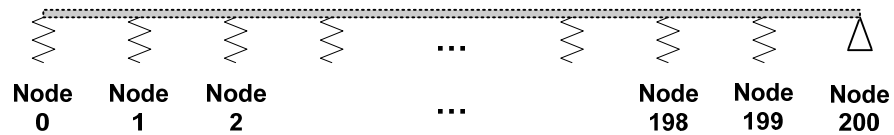


Figure 3. 17 Node Numbering in the Pipe when the Number of Element is 200

Assume a riser pipe hinged at the right-hand side and free at the left-hand side having 200 elements. The node number begins at 0 and the last node number is 200 upon hinged support like Figure 3.17. As mentioned in section 2.2, the finite difference equation can be following:

$$\frac{EI}{dx^4} [y_{i-2} - 4y_{i-1} + 6y_i - 4y_{i+1} + y_{i+2}] = -ky_i$$

A fourth-order differential equation requires specification of 4 boundary conditions. The first 2 equations are based on assumption of zero bending moment (zero curvature) at the supports. This is described in FD form as follows:

$$\text{For free end (M=0): } \frac{d^2y}{dx^2}(x=0) = 0 \rightarrow y_1 - 2y_0 + y_{-1} = 0 \quad (3.5)$$

$$\text{For hinged end (M=0): } \frac{d^2y}{dx^2}(x=L) = 0 \rightarrow y_{201} - 2y_{200} + y_{199} = 0 \quad (3.6)$$

y_0 and y_{200} in the equation 3.5 and 3.6 are substituted by the other boundary conditions ($y_0 = u$ and $y_{200} = 0$) stated in section 3.2.1.

$$y_{-1} = 2y_0 - y_1 \quad \text{and} \quad y_{201} = 2y_{200} - y_{199} \quad (3.7)$$

y_{-1} and y_{201} in the differential equation for each node is replaced by equation 3.7 as follows:

At node #1

$$\begin{aligned} \frac{EI}{dx^4} [y_{-1} - 4y_0 + 6y_1 - 4y_2 + y_3] &= -k \cdot y_1 \\ \left(5 + k \cdot \frac{dx^4}{EI} \right) \cdot y_1 - 4y_2 + y_3 &= 2u \end{aligned}$$

At node #2

$$\begin{aligned} \frac{EI}{dx^4} [y_0 - 4y_1 + 6y_2 - 4y_3 + y_4] &= -k \cdot y_2 \\ -4y_1 + \left(6 + k \cdot \frac{dx^4}{EI} \right) \cdot y_2 - 4y_3 + y_4 &= -u \end{aligned}$$

At node #3

$$\frac{EI}{dx^4} [y_1 - 4y_2 + 6y_3 - 4y_4 + y_5] = -k \cdot y_3$$

$$y_1 - 4y_2 + \left(6 + k \cdot \frac{dx^4}{EI}\right) \cdot y_3 - 4y_4 + y_5 = 0$$

At node # 198

$$\frac{EI}{dx^4} [y_{196} - 4y_{197} + 6y_{198} - 4y_{199} + y_{200}] = -k \cdot y_{198}$$

$$y_{196} - 4y_{197} + \left(6 + k \cdot \frac{dx^4}{EI}\right) \cdot y_{198} - 4y_{199} = 0$$

At node # 199

$$\frac{EI}{dx^4} [y_{197} - 4y_{198} + 6y_{199} - 4y_{200} + y_{201}] = -k \cdot y_{199}$$

$$y_{197} - 4y_{198} + \left(5 + k \cdot \frac{dx^4}{EI}\right) \cdot y_{199} = 0$$

Matrixes are made by these finite difference equations.

$$\begin{bmatrix} \left(5 + k \cdot \frac{dx^4}{EI}\right) & -4 & 1 & 0 & \dots & \dots & \dots & \dots & \dots & 0 \\ -4 & \left(6 + k \cdot \frac{dx^4}{EI}\right) & -4 & 1 & 0 & \dots & \dots & \dots & \dots & 0 \\ 1 & -4 & \left(6 + k \cdot \frac{dx^4}{EI}\right) & -4 & 1 & 0 & \dots & \dots & \dots & 0 \\ \dots & \dots & \dots & \dots & \dots & \dots & \dots & \dots & \dots & \dots \\ 0 & \dots & \dots & \dots & \dots & 0 & 1 & -4 & \left(6 + k \cdot \frac{dx^4}{EI}\right) & -4 \\ 0 & \dots & \dots & \dots & \dots & \dots & 0 & 1 & -4 & \left(5 + k \cdot \frac{dx^4}{EI}\right) \end{bmatrix} \begin{bmatrix} y_1 \\ y_2 \\ y_3 \\ \dots \\ y_{198} \\ y_{199} \end{bmatrix} = \begin{bmatrix} 2u \\ -u \\ 0 \\ \dots \\ 0 \\ 0 \end{bmatrix}$$

This equation of matrixes can be expressed as $[K][y] = [p]$. The deflection matrix $[y]$

is calculated by $[y] = [K]^{-1} [p]$.

Accuracy of FD Model

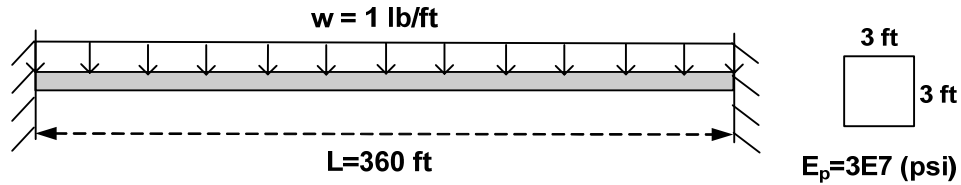


Figure 3. 18 Rectangular Beam Fixed Two Ends

The deflection at center for beam of two fixed ends with the distribution load as shown Figure 3.18 is

$$\delta_{\max} = \frac{wL^4}{384EI} = \frac{(1)(360)^4}{384(3 \times 10^7 \times 12^2)(3^4 / 12)} = 0.0015 \text{ (ft)}$$

Also, the bending moment is

$$M_{\text{end}} = \frac{wL^2}{12} = \frac{(1)(360)^2}{12} = 10800 \text{ (lb} \cdot \text{ft)}$$

Figure 3.19 and 3.20 are the result from simulating FE Model and FD Model. The analytical results agree well with the simulation results of FEA and FDA.

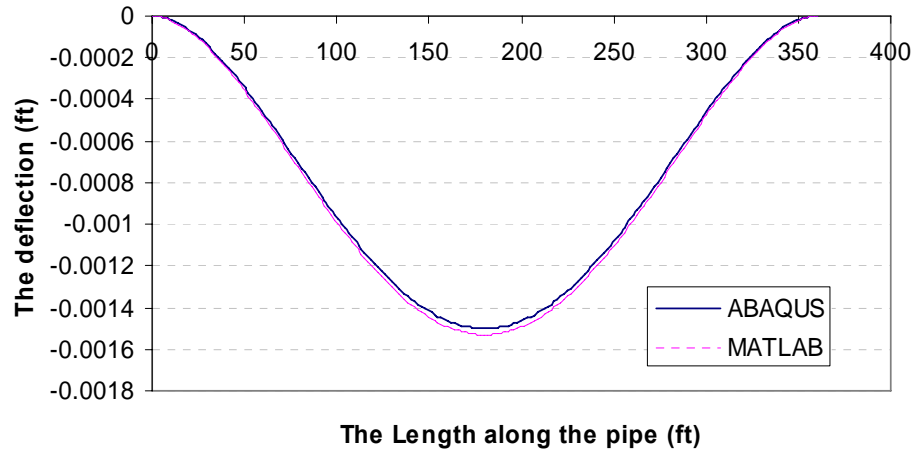


Figure 3. 19 Deflection Change along Pipe Length for Figure 3.18

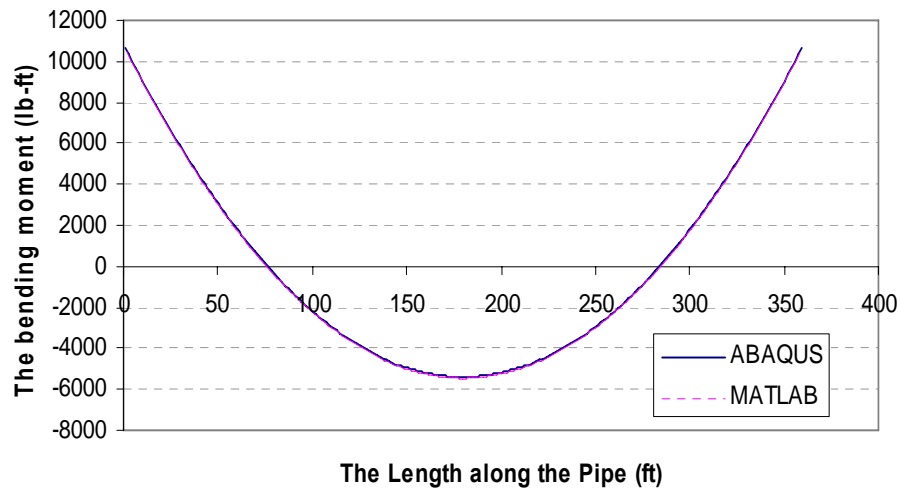


Figure 3. 20 Bending Moment Change along Pipe Length for Figure 3.18

Using the basic concept for FDM stated above, the basic features of the model with nonlinear spring include the following:

- Input variables include E , I , k_0 (F/L^2), P_{\max} and δ_y .
- Construct stiffness matrix of spring using the boundary conditions and differential equation stated earlier.

$$EI \left(\frac{y_{i-2} - 4y_{i-1} + 6y_i - 4y_{i+1} + y_{i+2}}{dx^4} \right) = -ky_i$$

- Perform the first iteration using the elastic spring constant (k_0) to compute deformation (δ).
- Determine equivalent spring constant (k) consistent with the deformation (δ) from the first iteration.
 - If the current deformation (δ) is larger than the yield deformation (δ_y), then update spring constant to secant spring constant ($k^* = P_{\max}/\delta$). Otherwise, if the present deformation (δ) is lower than the yield deformation (δ_y), use the initial spring constant (k_0).
- Iterate the previous step until $(\delta_i - \delta_{i-1})/\delta_{i-1}$ is lower than 0.01.
- Calculate the moment with the deflection results for each node.

$$M = -EI \left(\frac{y_{i-1} - 2y_i + y_{i+1}}{dx^2} \right)$$

- Calculate the bending stress,

$$\sigma_{bending} = \frac{Mc}{I}$$

where, c is the distance from the neutral axis to the outer edge of the beam.

Figure 3.21 shows the flow chart of FD model with nonlinear soil spring.

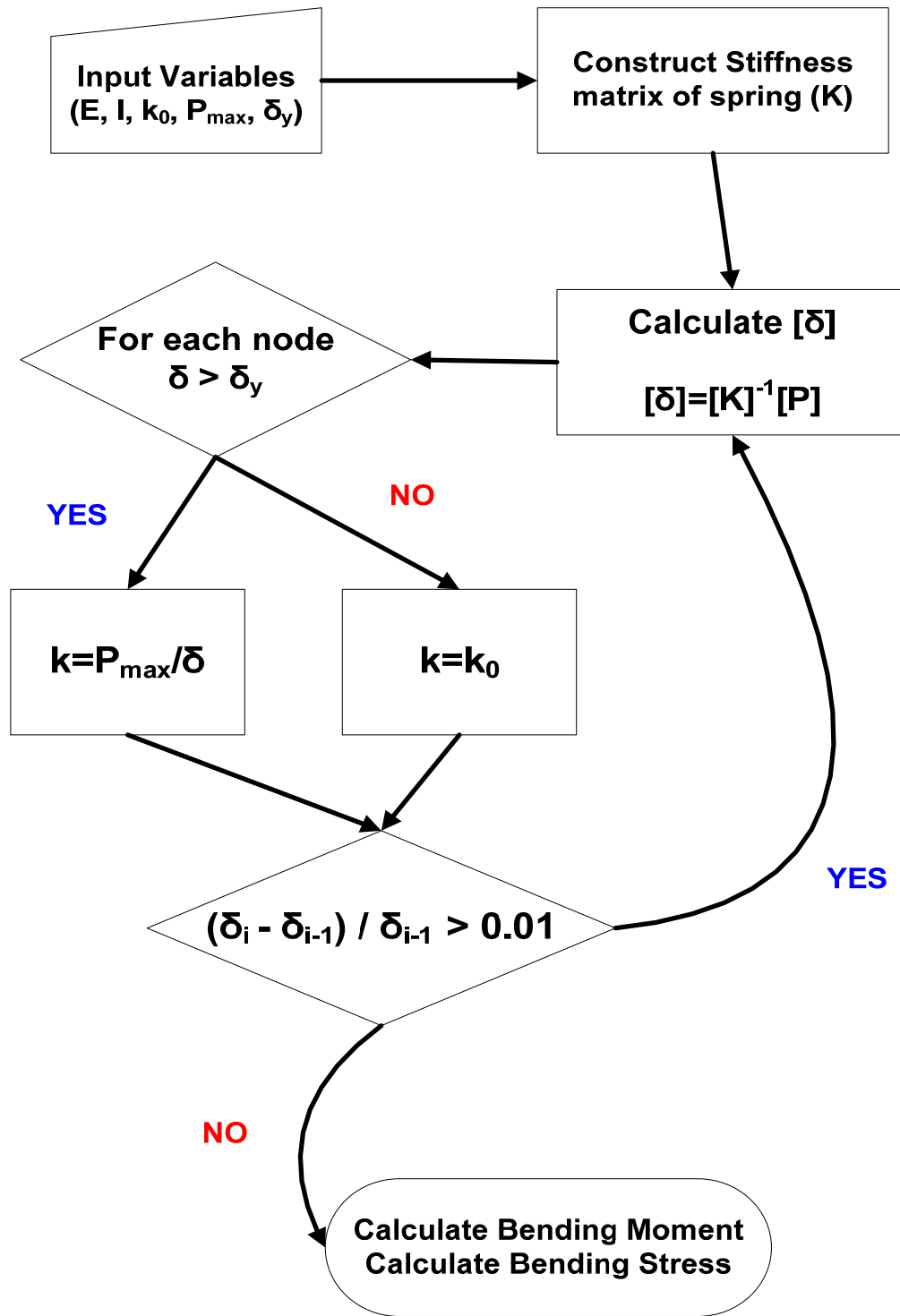


Figure 3. 21 Flow Chart of FD Model with Nonlinear Soil Spring

3.3.2 FD Model with Linear Spring

As illustrated in Figure 3.22, soil spring stiffness (k_0) is constant and its unit is force per square length. Up-load displacement is equal to down-load displacement. Because of influence of linear spring, the foundation support force increases without limit with increasing relative displacement in proportion to the spring constant. Figure 3.23 show good agreement between FE and FD result. The input data in Table 3.3 is used for all figures in the FD model section.

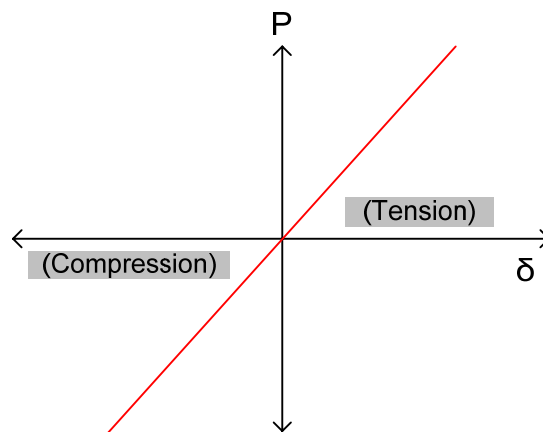


Figure 3. 22 P- δ Curve of Linear Spring

Table 3. 3 Input Data for Figures in Section 3.3 ($E_s/S_u=100$, $H/D=1.0$, $W/D=1.0$)

L (in)	dx (in)	E_p (ksi)	D (in)	t (in)	S_u (psi)	$[P_{max}]_{norm}$ (lb/in)	$[k_0]_{norm}$ (psi)	$[\delta_y]_{norm}$ (in)	u (in)
3600	18	30,000	6	0.5	1	6.4	272	0.0235	1

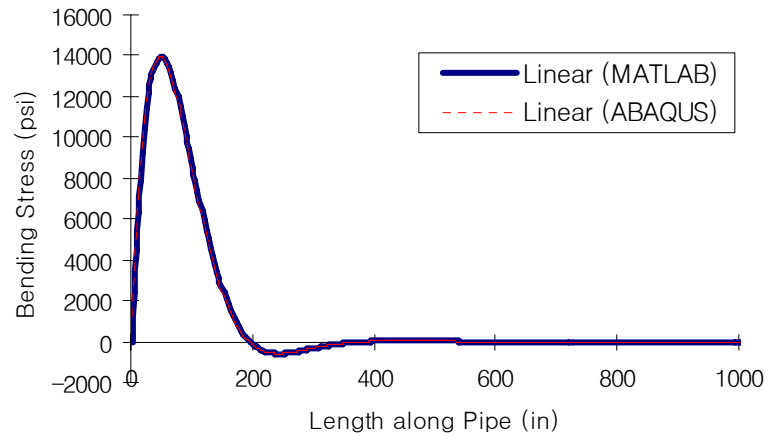


Figure 3. 23 Comparison between FEA and FDA for Bending Stress along Pipe Length

3.3.3 FD Model with Nonlinear Spring

The soil spring shows linear elastic behavior under δ_y , but it will behave nonlinear if a relative deformation excesses δ_y unlike linear spring. Under perfectly plastic state, the initial spring constant is substituted as secant modulus k which is calculated from P_{\max} divided by δ_y . Figure 3.24 shows the nonlinear spring and Figure 3.25 illustrates the result for comparison between FE and FD model with nonlinear spring.

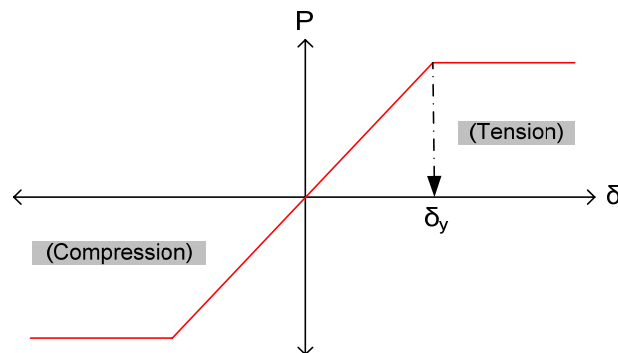


Figure 3. 24 P- δ Curve of Nonlinear Spring

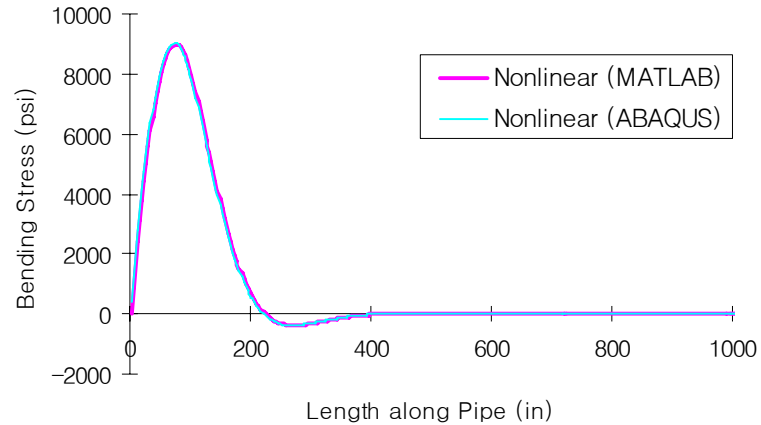


Figure 3. 25 Comparison between FEA and FDA for Bending Stress along Pipe Length

3.3.4 FD Model with Tension Cut-off Spring

In reality, the seafloor can support the riser pipe when the riser motion was downward after the riser pipe contacts with the seafloor. Otherwise, when the riser pipe moves up from the seafloor, the soil spring which represents the seafloor would disappear directly or after applied load passes over a value of load due to the effect of a pipe pulling out of contact with the soil such as Figure 3.26. In the model, a tension cut-off parameter (t_{co}) is defined by the ratio of the maximum load in tension to that in compression such as 10%, 50%, and 100%.

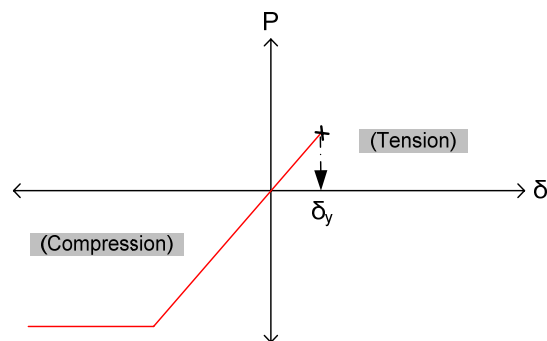


Figure 3. 26 P- δ Curve of Tension Cut-off Spring

3.3.5 FDM Results

As showed in Figure 3.27 and 3.28, the maximum bending stress decreases depending on the degree of model development for different kinds of soil spring. It is because the characteristic of each P- δ curve appear on the bending stress values. In addition, the tension cut-off parameter (t_{co}) affects on the maximum bending stress and the distribution of bending stress along the pipe as illustrated in Figure 3.29 and 3.30.

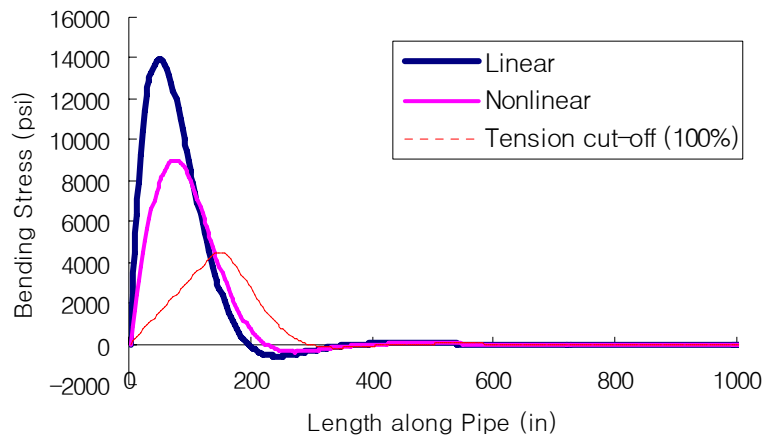


Figure 3. 27 Bending Stress for Variable Types of Soil Spring

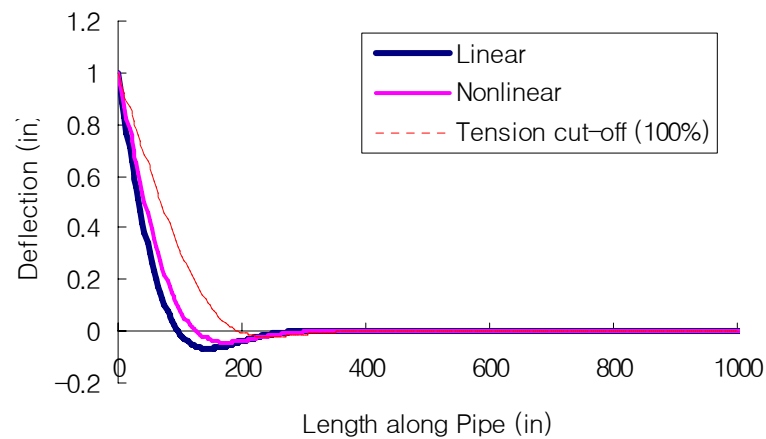


Figure 3. 28 Deflection for Variable Types of Soil Spring

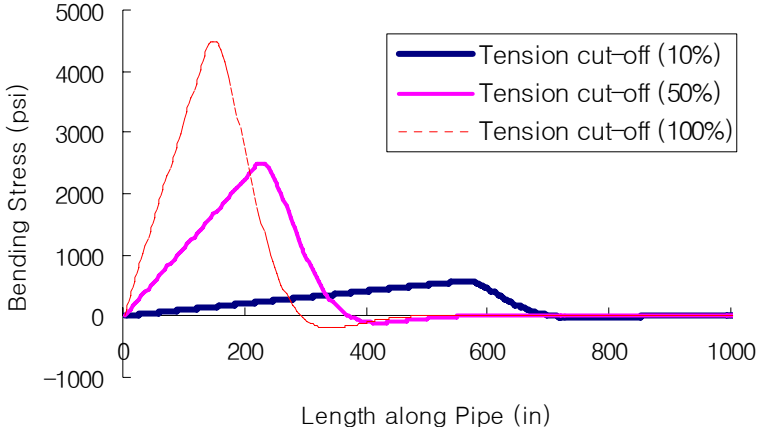


Figure 3. 29 Bending Stress Variation for Influence of t_{co}

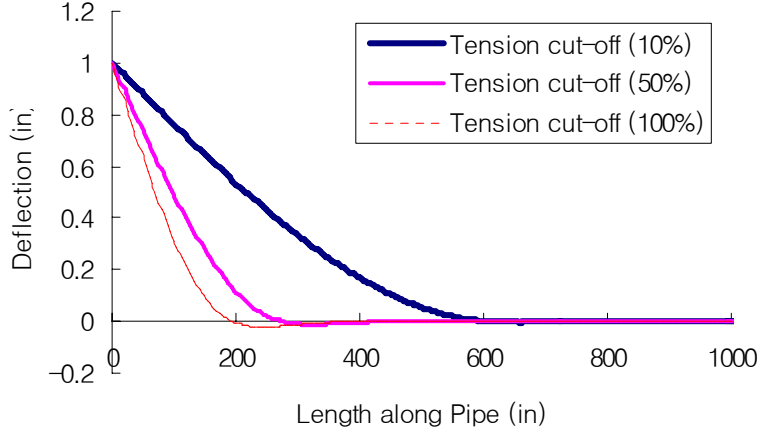


Figure 3. 30 Deflection Variation for Influence of t_{co}

CHAPTER IV

PARAMETRIC STUDIES

4.1 INTRODUCTION

The main factors to control the magnitude of bending stress in the riser pipe are riser movement characteristics, seafloor stiffness, and touchdown zone characteristics. Parametric studies relevant to these factors were conducted with the pipe-nonlinear soil spring support model as shown Figure 4.1.

The length of riser pipe (L) is 300ft (3600in) and the number of elements in the model is 200 except section 4.5. The properties of riser pipe are like following: the modulus of pipe (E_p) is 30,000ksi, the yield stress of pipe (σ_y) is 60ksi, the diameter of pipe (D) is 6in, and the thickness of pipe (t) is 0.5in. In addition, the only case for trench width to diameter of pipe, $W/D=1.0$, was simulated because this simplified model do not consider the lateral soil spring effect.

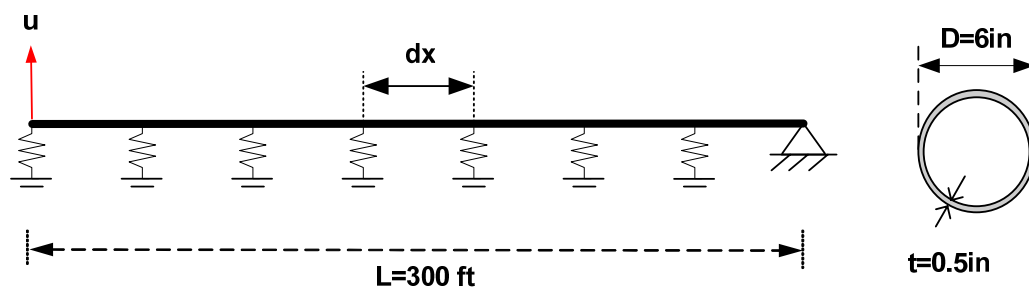


Figure 4. 1 Pipe-Nonlinear Soil Spring Support Model

4.2 LOAD-DEFORMATION (P- δ) CURVE CHARACTERISTICS

The broad limits on the range of P- δ curves associated with various condition of seafloor stiffness were considered in this parametric study. For example, the ratio for embedment depth of pipe to the diameter of the riser pipe (H/D), the width of trench to the diameter of the riser pipe (W/D), the soil modulus to the undrained shear strength of soil (E_s/S_u) were considered in P- δ curves. It should be noted that spring stiffness can be varied along the length of the pipe to simulate variable trench depth conditions. Table 4.1 shows the values for each ratio.

Table 4. 1 Range of Ratio for H/D, E_s/S_u (W/D=1.0)

E_s/S_u	H/D	k_{norm}	$(P_{max})_{norm}$	$(\delta_y)_{norm}$
100	0.5	237	5.70	0.0240
	1.0	272	6.40	0.0235
	2.0	321	7.19	0.0224
	3.0	331	7.82	0.0236
	4.0	331	8.25	0.0249
500	0.5	1072	5.70	0.00532
	1.0	1167	6.42	0.00550
	2.0	1237	7.22	0.00584
	3.0	1263	7.85	0.00622
	4.0	1536	8.30	0.00540
1000	0.5	2366	5.70	0.00241
	1.0	2705	6.42	0.00237
	2.0	3013	7.22	0.00240
	3.0	3080	7.85	0.00255
	4.0	3072	8.30	0.00270
1500	0.5	3443	5.70	0.00166
	1.0	3791	6.42	0.00169
	2.0	4052	7.22	0.00178
	3.0	4138	7.86	0.00190
	4.0	4129	8.30	0.00201

Figure 4.2 illustrates influence of E_s/S_u on elastic stiffness in the normalized P- δ curve for conditions of $W/D=1.0$ and $H/D=0.5$. It shows that the normalized soil spring constant (k_{norm}) is increasing by increasing ratio of E_s/S_u .

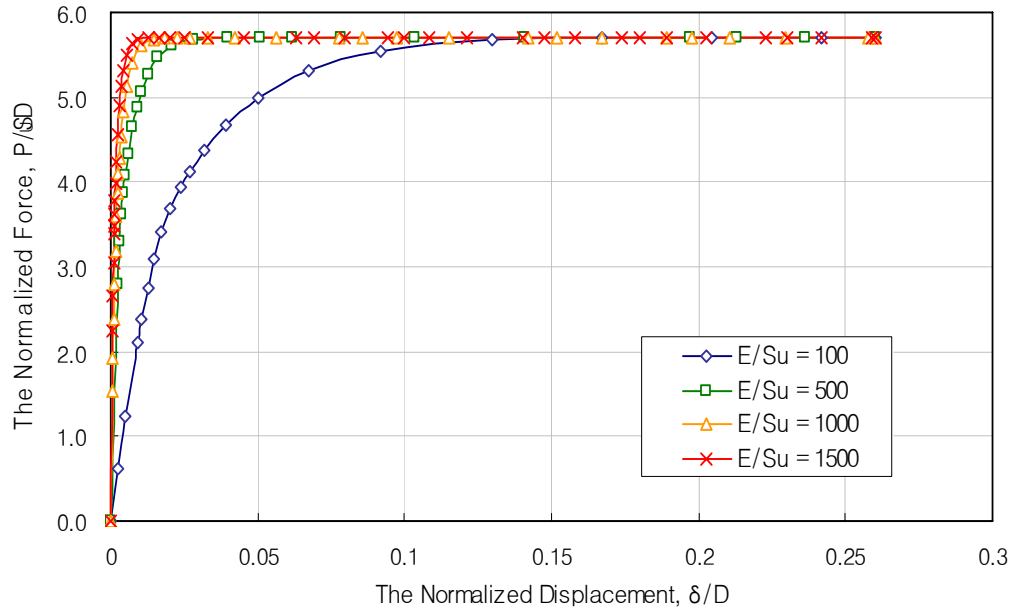


Figure 4. 2 Effect of E_s/S_u on Elastic Stiffness ($H/D=0.5$)

Figure 4.3 shows the deflection along the pipe made from simulating the simplified model (Fig. 4.1) with conditions of E_s/S_u ranging from 100 to 1500, $H/D=1.0$, $S_u=1$ (psi), and $u=1$ (in). The higher value of E_s/S_u has a little bit bigger curvature. Otherwise, the smaller ratio of E_s/S_u makes a little longer touch down zone.

Figure 4.4 illustrates the bending stress change along the pipe length with same conditions with Fig. 4.3. The maximum bending stress for $E_s/S_u = 1000$ is a little bigger than others. However, the point which occur the maximum bending stress looks similar for each other.

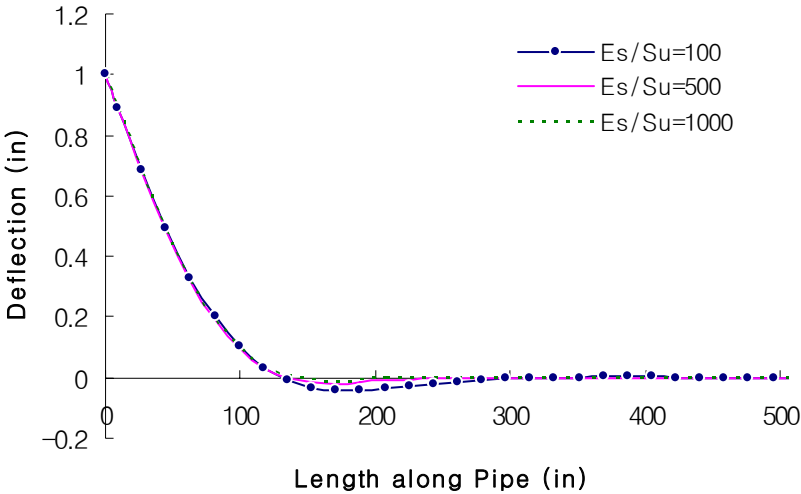


Figure 4. 3 Deflection Change along Pipe Length for Various E_s/S_u ($H/D=1.0$, $u=1$ in)

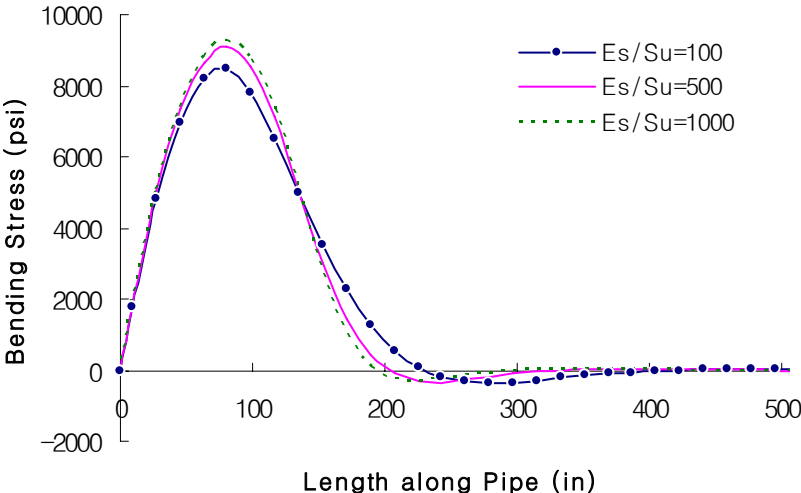


Figure 4. 4 Bending Stress Change along Pipe Length for Various E_s/S_u ($H/D=1.0$, $u=1$ in)

Figure 4.5 shows effect of trench depth in the normalized P- δ curves for conditions of $W/D=1.0$ and $E_s/S_u=100$. This illustrates positive correlation between the normalized force and the ratio, H/D .

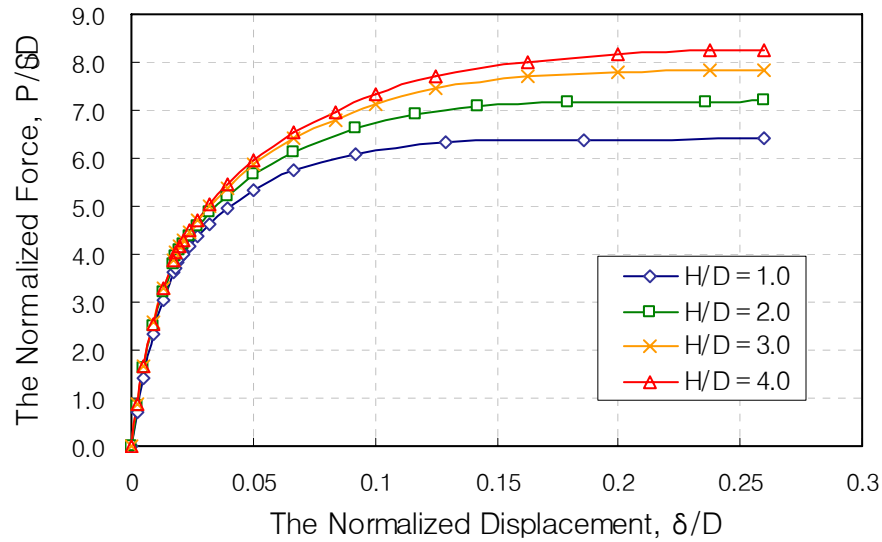


Figure 4. 5 Effect of Trench Depth ($E_s/S_u=100$)

Figure 4.6 illustrates the deflection change along the riser pipe for the various H/D ranging from 1.0 to 4.0 with conditions of $E_s/S_u=100$, $S_u=1$ (psi), and $u=1$ (in). The deeper trench embedment has a little bit higher curvature.

Figure 4.7 shows the bending stress change along the riser pipe with same conditions with Figure 4.6. The maximum bending stress is increasing when the pipe embedment is deeper.

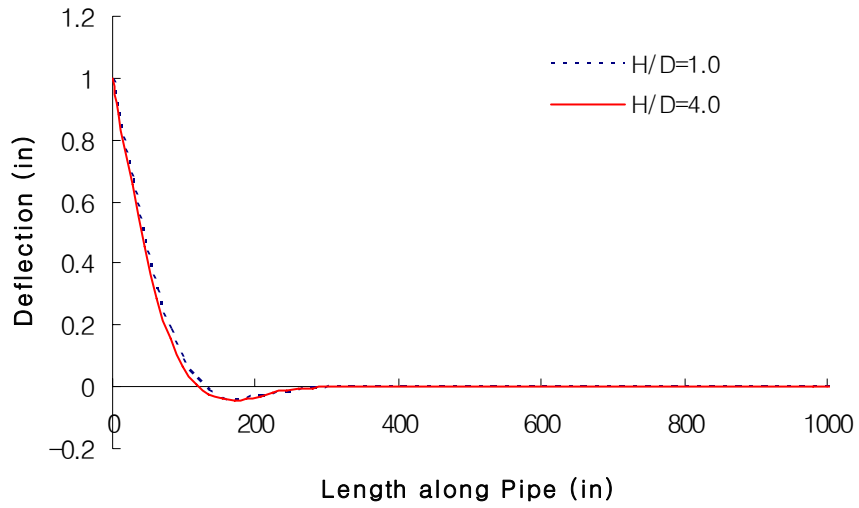


Figure 4. 6 Deflection Change along Pipe Length for Various H/D (H/D=1.0, $u=1$ in)

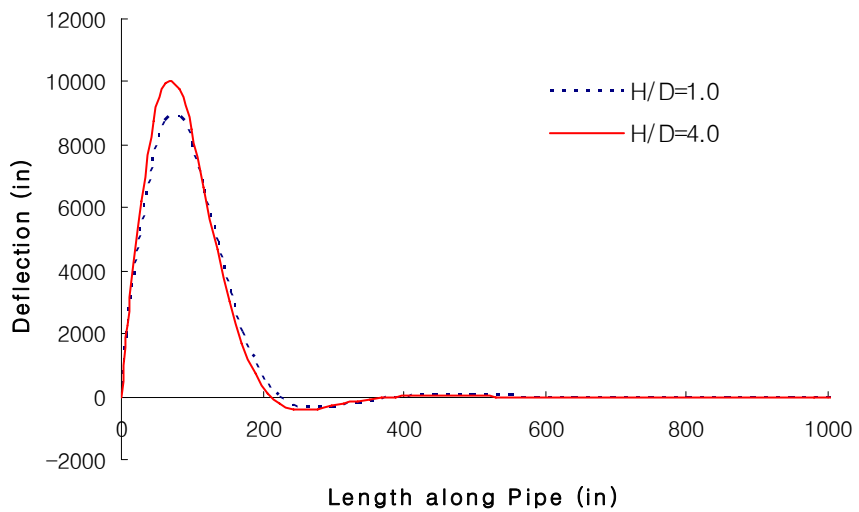


Figure 4. 7 Bending Stress Change along Pipe Length for Various H/D (H/D=1.0, $u=1$ in)

Finally, Figure 4.8 shows effect of trench width in the normalized P- δ curves for conditions of $H/D=1.0$ and $E_s/S_u=100$. It illustrates that the wider trench width make the normalized force reduced. This result would be because of the effect of soil softening.

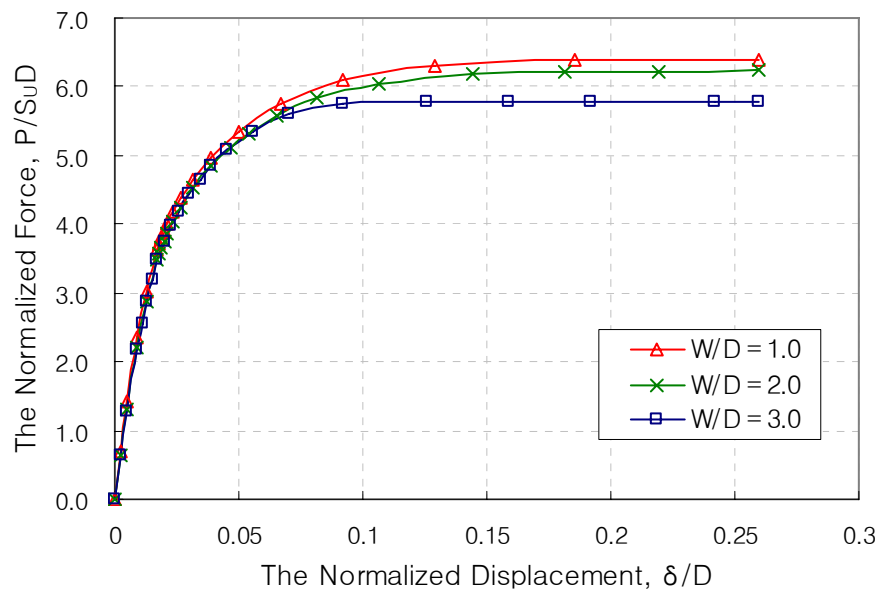


Figure 4. 8 Effect of Trench Width ($H/D=1.0$, $E_s/S_u=100$)

4.3 SOIL TO PIPE STIFFNESS

The soil stiffness is one of significant factors which affect the bending stress in the riser pipe. The each ratio such as H/D , E_s/S_u and W/D can change soil stiffness in the simplified model. Therefore, this section focuses on the change of the maximum bending stress in riser pipe depend on the variation of normalized parameter such as the relative stiffness of pipe and soil ($k_0 D^4/E_p I$); here, the unit of k_0 is force per square length. The modulus of soil is calculated from multiplying the ratio, E_s/S_u , by S_u .

The parameter, $\lambda = k_0 D^4/E_p I$, describes the ratio of soil stiffness to pipe stiffness. Pipe stiffness is conveniently expressed in terms of pipe modulus (E_p) and moment of inertia (I), the soil stiffness (k_0) is a function of a series of soil and trench geometry variables, including E_s/S_u , H/D , W/D . For this study, only $W/D=1$ was considered.

In performing a parametric study on the effects of k_0 , a range of soil moduli $E_s/S_u=100\sim 1500$ was considered, and a range of trench depths $H/D=0.5\sim 4.0$ was considered. k_0 and λ based on these ranges of parameters are as following tables 4.2 and 4.3.

Table 4. 2 A Range of k_0 (psi) Depend on the Ratio H/D and E_s/S_u ($S_u=1$ psi)

H/D \ Es/Su	100	500	1000	1500
0.5	237	1072	2366	3443
1.0	272	1167	2705	3791
2.0	321	1237	3013	4052
3.0	331	1263	3080	4138
4.0	331	1536	3072	4129

Table 4. 3 A Range of λ Depend on the Ratio H/D and E_s/S_u ($S_u=1$ psi)

H/D \ Es/Su	100	500	1000	1500
0.5	0.000311	0.00141	0.00310	0.00452
1.0	0.000357	0.00153	0.00355	0.00497
2.0	0.000421	0.00162	0.00395	0.00531
3.0	0.000434	0.00166	0.00404	0.00543
4.0	0.000434	0.00201	0.00403	0.00542

Based on this range of k-values predicted bending stress $(\sigma_b)_{\max}/\sigma_y$ for various conditions of soil to pipe stiffness are shown in Figure 4.9.

Figure 4.9 illustrates the relation between $(\sigma_b)_{\max}/\sigma_y$ and λ depends on various H/D ranging from 0.5 to 4.0 for conditions of E_s/S_u is 100, S_u ranging from 0.25 to 7.0 (psi), E_s ranges from 25 to 700 (psi), and u is 1in.

Figure 4.10 indicates the relation between the maximum bending stress to the yield stress, $(\sigma_b)_{\max}/\sigma_y$, and λ depend on various E_s/S_u ranging from 100 to 1500 for conditions of H/D=1.0, S_u ranging from 0.25 to 7.0 (psi), and $u=1$ (in). E_s has the following ranges; 25~700, 125~3500, 250~7000, and 375~10500 (psi) for each ratio of E_s/S_u .

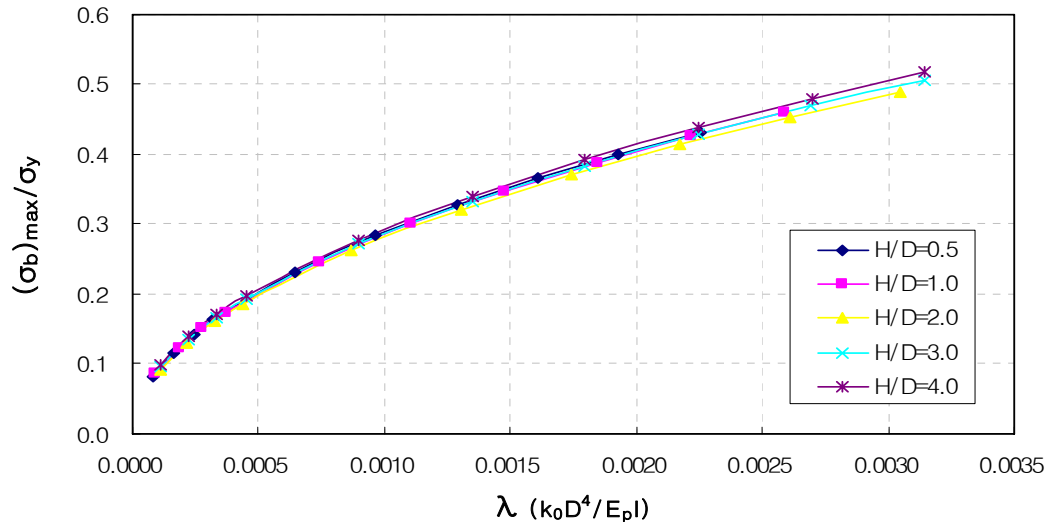


Figure 4. 9 Effect of Ratio for Variable Ratio λ ($W/D=1.0$, $u=1$ in)

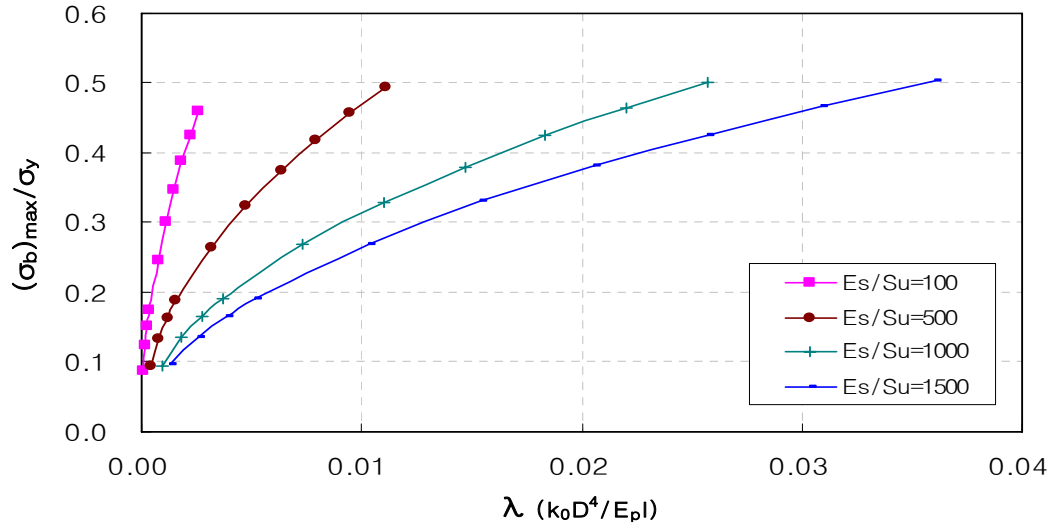


Figure 4. 10 Effect of Ratio E_s/S_u for Variable Ratio λ ($H/D=1.0$, $u=1$ in)

Figure 4.11 shows the deflection change along the riser pipe for the various S_u ranging from 0.25 to 7.0 (psi) with conditions of $H/D=1.0$, $E_s/S_u=100$, and $u=1$ (in). The higher undrained shear strength gets the higher curvature when the up-ward displacement occurs. In addition, the TDP moves to left side by increasing S_u and the buried zone of riser pipe is shorter.

Figure 4.12 shows the bending stress change along the riser pipe with same conditions with Fig. 4.11. The maximum bending stress is gone up by increasing S_u and moves to the origin in the coordinate.

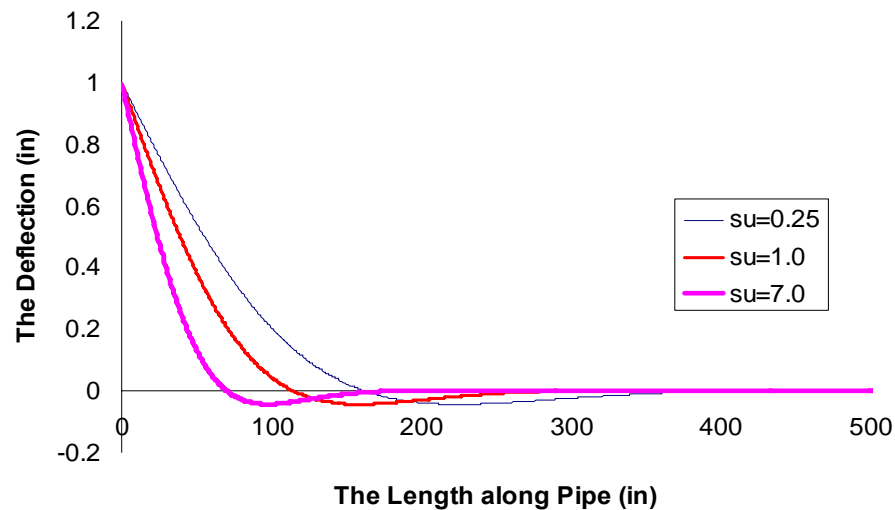


Figure 4. 11 Deflection Change along Pipe Length for Various S_u ($H/D=1.0$, $E_s/S_u=100$, $u=1$ in)

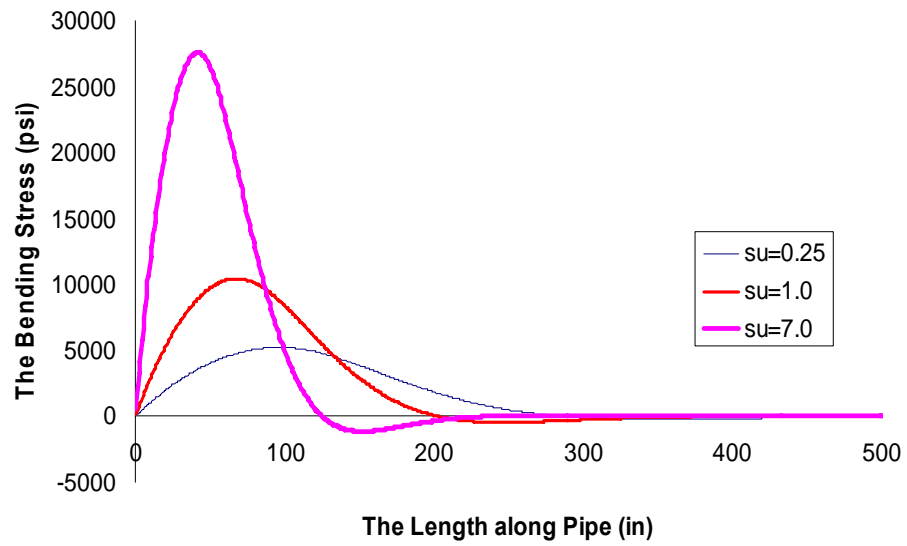


Figure 4. 12 Bending Stress Change along Pipe Length for Various S_u ($H/D=1.0$, $E_s/S_u=100$, $u=1$ in)

4.4 AMPLITUDE OF STEEL CATENARY RISER MOTIONS

The SCR-seafloor behavior can be strongly influenced by the amplitude of riser motions around the touchdown zone. Thus, the amplitude of riser motions can affect yielding of the soil as well as the bending stress in riser pipe. As a simple example, large amplitude riser motions can lead to formation of a trench in the seafloor that can considerably increase the effective resistance of the seafloor to riser movements. Tables 4.4 and 4.5 show the range of δ_y and u/δ_y based on the Ratio H/D and E_s/S_u .

Table 4. 4 A Range of δ_y (in) Depend on the Ratio H/D and E_s/S_u

E_s/S_u		100	500	1000	1500
H/D					
0.5		0.144	0.0319	0.0145	0.0100
1.0		0.141	0.0330	0.0142	0.0101
2.0		0.134	0.0350	0.0144	0.0107
3.0		0.142	0.0373	0.0153	0.0114
4.0		0.149	0.0324	0.0162	0.0121

Table 4. 5 A Range of u/δ_y Depend on the Ratio H/D and E_s/S_u

$u = 1$ in		E_s/S_u			
H/D		100	500	1000	1500
0.5		6.94	31.3	69.2	100
1.0		7.09	30.3	70.3	98.6
2.0		7.44	28.5	69.4	93.6
3.0		7.06	26.8	65.4	87.7
4.0		6.69	30.9	61.7	82.9
$u = 6$ in		E_s/S_u			
H/D		100	500	1000	1500
0.5		42	188	415	602
1.0		43	182	422	592
2.0		45	171	417	562
3.0		42	161	392	526
4.0		40	185	370	498
$u = 12$ in		E_s/S_u			
H/D		100	500	1000	1500
0.5		83	376	830	1205
1.0		85	364	844	1183
2.0		89	342	833	1124
3.0		85	322	784	1053
4.0		80	370	741	995

Figure 4.13 illustrates the maximum bending stress is going up when the ratios, λ and u/δ_y increase. Based on this range of k_0 values as mentioned before, predicted bending stress $(\sigma_b)_{\max}/\sigma_y$ for various conditions of soil to pipe stiffness use shown in the figure. The influence of magnitude of riser motion is much more significant than the one of pipe embedment depth as shown in the fig.

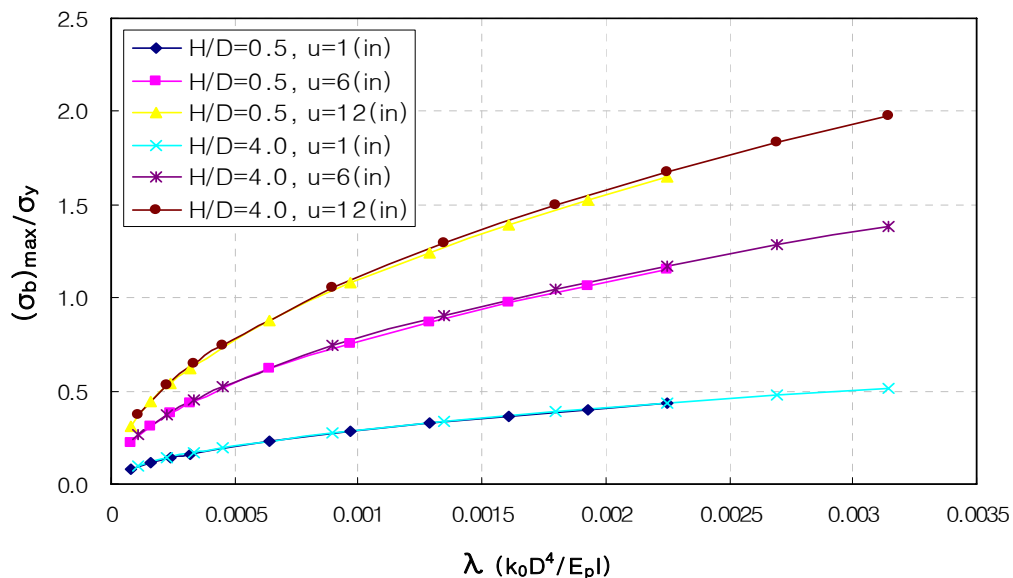


Figure 4. 13 Effect of Displacement of Pipe for Variable Ratio λ ($W/D=1.0$, $E_s/S_u=100$)

Figure 4.14 shows the deflection change along the riser pipe for the various displacement, u ranging from 0.25 to 7.0 (psi), with conditions of $H/D=1.0$, $E/S_u=100$, and $S_u=1$ (psi). The higher amplitude of loading makes much higher curvature. In addition, TDP move to right-side by increasing magnitude of loading.

Figure 4.15 illustrates the bending stress change along the riser pipe. The maximum bending stress is gone up by increasing magnitude of loading and moves to opposite direction to the origin in the coordinate.

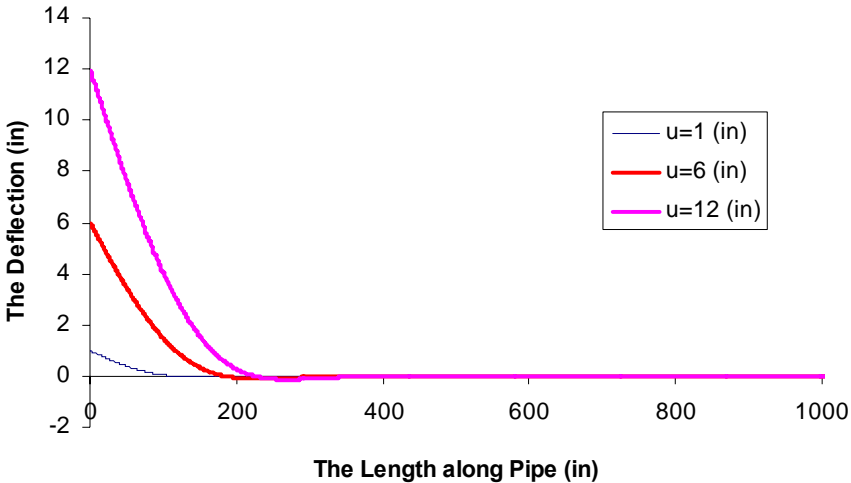


Figure 4. 14 Deflection Change along Pipe Length for Various Displacement, u (W/D=1.0, E/Su=100)

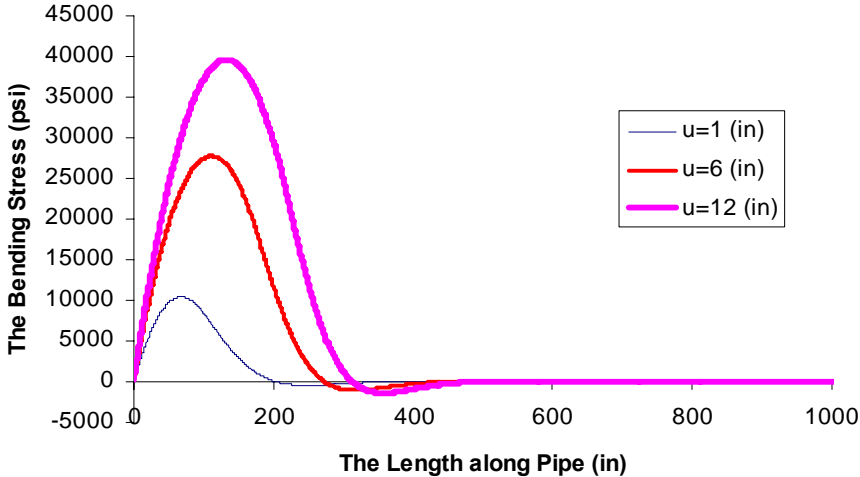


Figure 4. 15 Bending Stress Change along Pipe Length for Various Displacement, u (W/D=1.0, E/Su=100)

CHAPTER V

SUMMARY, CONCLUSIONS, AND RECOMMENDATIONS

5.1 SUMMARY AND CONCLUSIONS

The interaction between steel catenary risers and the seafloor involves a number of complexities including non-linear soil behavior, soil yielding, softening of seafloor soils under cyclic loading, variable trench width and depth, a wide range of possible riser displacement amplitudes, and conditions in which the riser pipe can actually pull out of contact with the soil. With a view toward making this complex problem more tractable, this research adopts a simplified model comprised of a riser pipe supported on a series of equivalent soil springs. The problem is then investigated through two sets of parallel studies:

1. Models for equivalent soil springs are developed based on two-dimensional finite element studies of a pipe embedded in a riser trench. In the long-term, soil spring models will be developed for various conditions of trench depth, trench width, soil elastic modulus, soil shear strength, trench backfill, and soil softening under cyclic loading. At the present time, only trench depth, soil elastic modulus, and trench width, that of the trench width equaling the pipe diameter. These studies were performed independently of the work presented in this thesis (Sharma, 2005), and the parametric studies presented in this thesis utilize the final product of that research effort.
2. Soil-pipe interactions are modeled through one-dimensional studies of a spring-

supported pipe subjected to displacements at one end of the pipe. Development of this model is a primary focus of this research. Primary outputs from this model include the deflected shape of the riser pipe, bending moments, and maximum bending stresses.

Direct inputs into the soil-pipe interaction model include parameters to characterize the soil springs, the riser pipe, the length of the touchdown zone, and the amplitude of imposed displacements.

A simple bi-linear model is used to characterize the springs. For loads (force per unit length) below a certain maximum, P_{\max} , the spring is linear and is described by a spring constant, k . When the load P_{\max} is reached, the spring resistance remains constant at P_{\max} and independent of the magnitude of deformation. In the case of tension (uplift), the model recognizes the possibility that the riser pipe can pull out of contact with the soil, in which case the riser-soil contact force declines to zero. A tension cutoff parameter, t_{co} , is introduced to express the ratio of the maximum load in tension to that in compression. In summary, three parameters describe the soil springs, k , P_{\max} , and t_{co} . It is noted that these parameters are a function of soil stiffness and strength properties, and trench geometry.

However, soil properties and trench geometry are indirect rather than direct inputs into the simplified model. It is possible to specify variable spring constants along the length of the pipe to simulate variable conditions of pipe embedment, although this option was not utilized in the parametric studies performed in this research.

The riser pipe input parameters include the elastic modulus of the pipe material (usually steel), pipe diameter, and the moment of inertia of the pipe cross-section. The pipe is modeled as a linearly elastic material.

The amplitude of imposed motions is specified as a single vertical displacement. The imposed displacement can be either upward or downward. Similarly, the length of the touchdown zone is specified as a single horizontal distance.

The preliminary studies performed in this study indicate the following:

1. The seafloor stiffness (as characterized by the three spring parameters), the magnitude of pipe displacement, and the length of the touchdown zone all influence bending stresses in the pipe and should be considered in future studies.
2. The tension cutoff effect, i.e., the pipe pulling away from the soil, can have a very large effect on bending stresses in the pipe. Neglecting this effect can lead to serious over-estimate of stress levels and excessive conservatism in design.

5.2 RECOMMENDATIONS FOR FUTURE RESEARCH

Topics for future research include the following:

1. Repeated load cycles can lead to remolding and softening of the seafloor soils. This will lead to reduced effective seafloor spring stiffness with reduced levels of bending stresses in the pipe. This effect can be particularly important for cases of stiff seafloor soils where remolding is likely to lead to substantial reductions in stiffness.
2. The current research only considers vertical pipe motions. Actual pipe motions

include a lateral component, the effects of which should be considered.

3. Displacement magnitudes are clearly critical to pipe bending stresses. This study considered a general range of displacements which risers are likely to experience.
4. The tension cutoff is clearly important. Future studies should address how an appropriate value for the tension cutoff should be estimated.
5. The riser pipe is not a straight line, but has a curved shape. The existing soil-riser interaction model should be modified to accommodate curved riser configurations.

REFERENCES

Boresi, A.P. and Schmidt, R.J. (2002). *Advanced mechanics of materials*, 6th Ed., Wiley, New York.

Bridge, C. and Willis, N. (2002). “Steel catenary risers – results and conclusions from large scale simulations of seabed interactions” *Proc., Int. Conf. on Deep Offshore Technology*, New Orleans, Louisiana, [〈http://www.2hoffshore.com/papers/docs/new/Paper64.pdf〉](http://www.2hoffshore.com/papers/docs/new/Paper64.pdf).

Bridge, C., Howells, H., Toy, N., Parke, G., and Woods, R. (2003). “Full scale model tests of a steel catenary riser” *Proc., Int. Conf. on Fluid Structure Interaction*, Cadiz, Spain, [〈http://www.2hoffshore.com/papers/docs/new/pap68.pdf〉](http://www.2hoffshore.com/papers/docs/new/pap68.pdf).

Bridge, C., Laver, K., Clukey, Ed., and Evans, T. (2004). “Steel catenary riser touchdown point vertical interaction models” *Proc., Conf. on Offshore Technology*, Houston, Texas, [〈http://www.2hoffshore.com/papers/docs/new/pap80.pdf〉](http://www.2hoffshore.com/papers/docs/new/pap80.pdf).

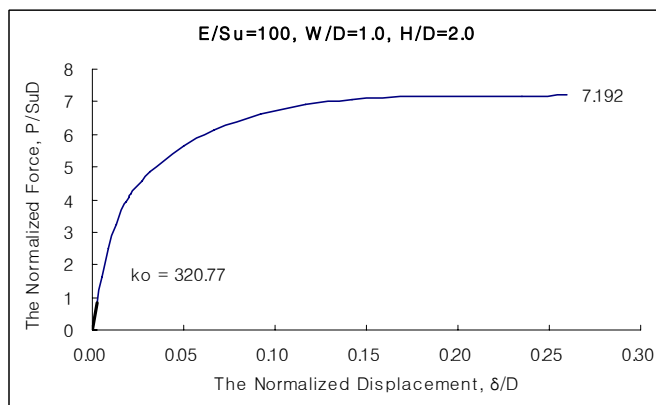
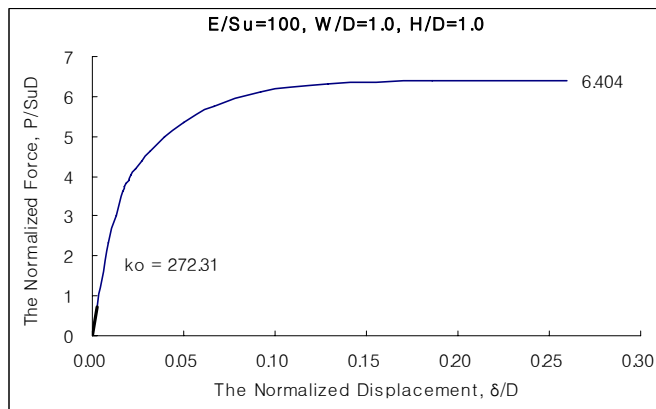
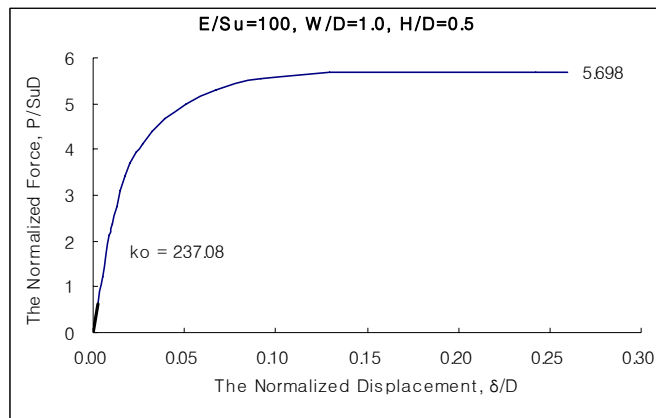
Desai, C.S. and Christian J.T. (1977), *Numerical methods in geotechnical engineering*, McGraw-Hill, New York.

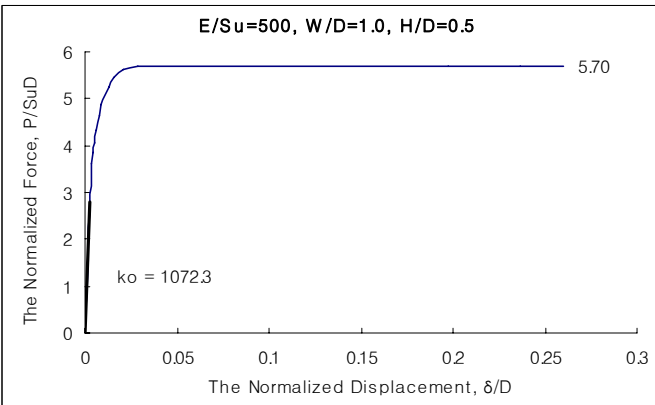
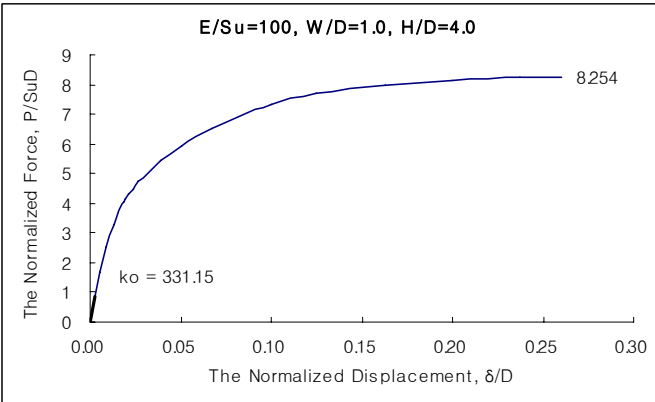
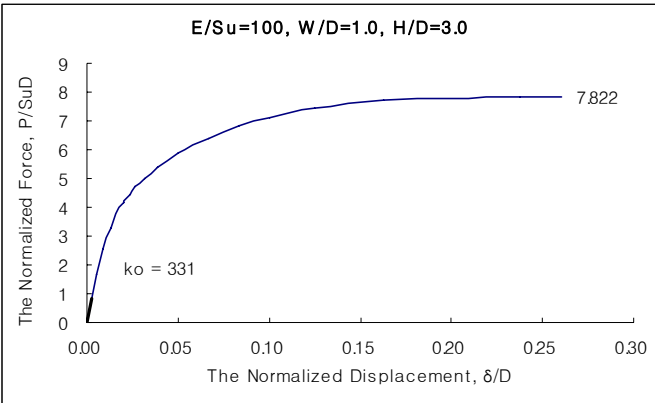
Pesce, C.P., Aranha, J.A.P., and Martins, C.A. (1998). “The soil rigidity effect in the touchdown boundary-layer of a catenary riser: static problem” *Proc., 8th Int. Conf. on Offshore and Polar Engineering*, Montreal, Canada, 2, 207-213

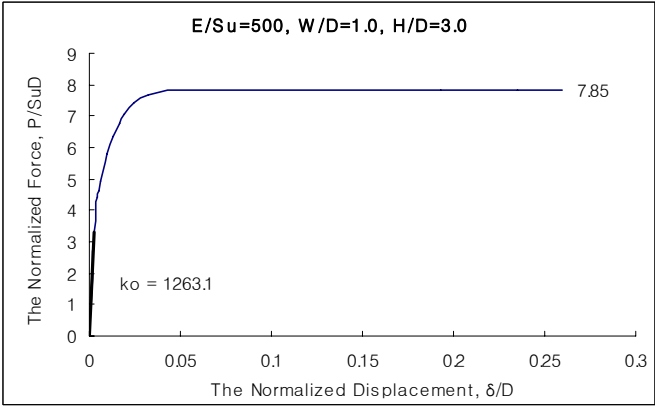
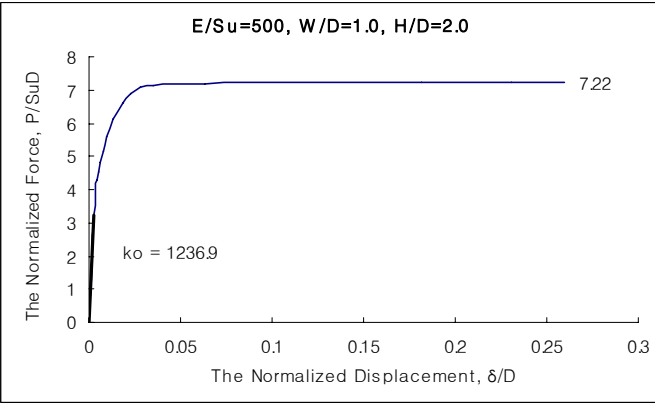
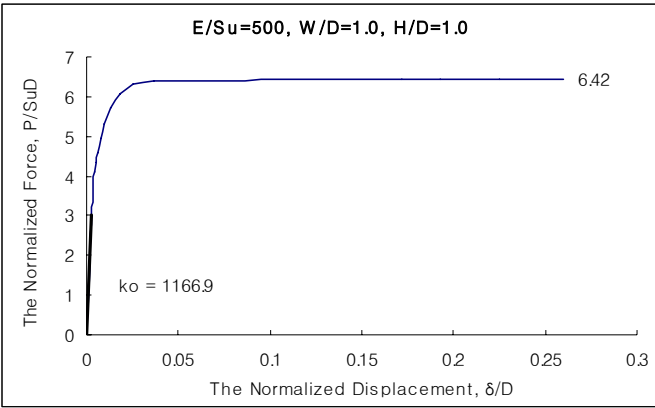
Thethi, R. and Moros, T. (2001). “Soil interaction effects on simple catenary riser response” *Proc., Conf. on Deepwater Pipeline & Riser Technology*, Houston, Texas, [〈http://www.2hoffshore.com/papers/docs/pap050.pdf〉](http://www.2hoffshore.com/papers/docs/pap050.pdf).

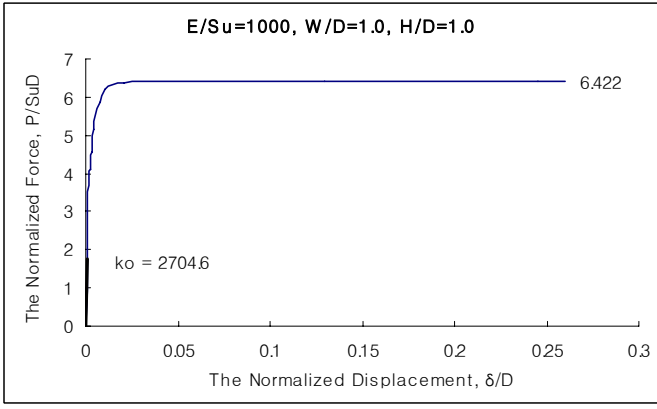
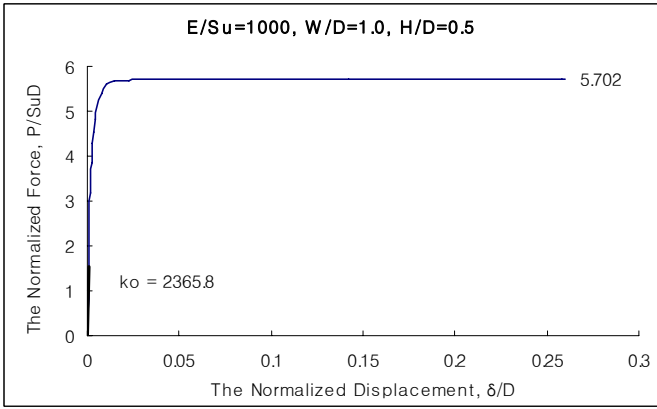
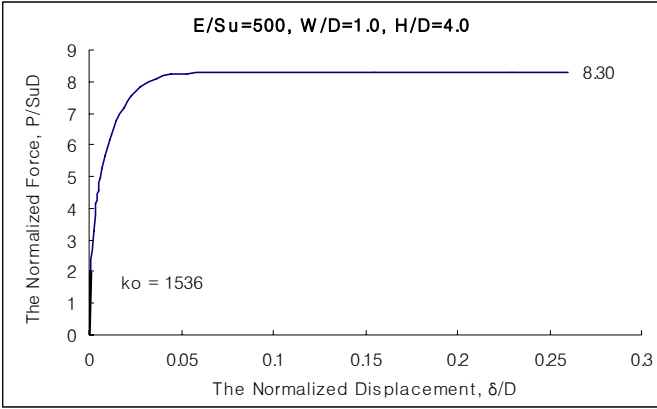
Willis, N.R.T and West, P.T.J (2001). “Interaction between deepwater catenary risers and a soft seabed: Large scale sea trials” *Proc., Conf. on Offshore Technology*, Houston, Texas, [〈 http://www.2hoffshore.com/papers/docs/pap048.pdf 〉](http://www.2hoffshore.com/papers/docs/pap048.pdf).

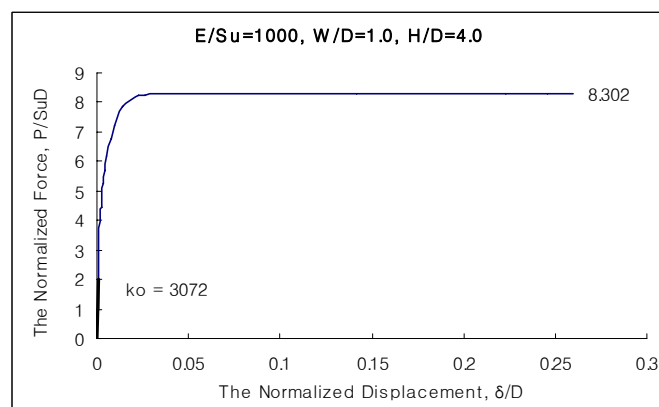
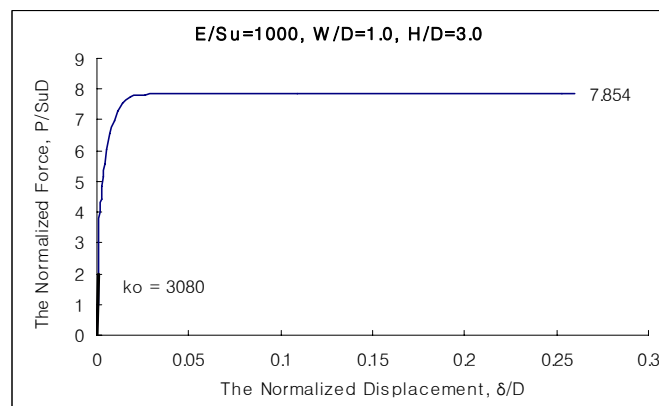
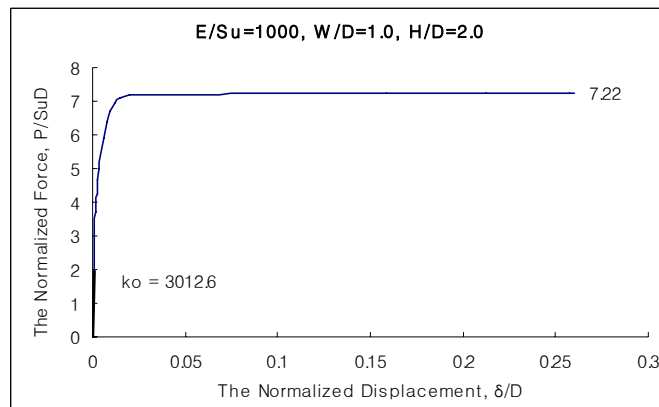
APPENDIX A
NORMALIZED LOAD-DEFORMATION CURVES

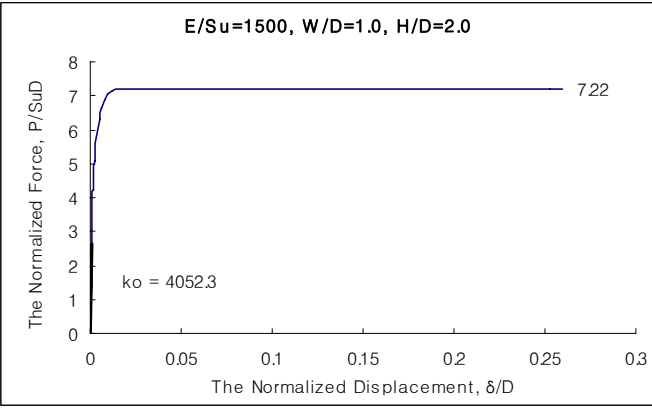
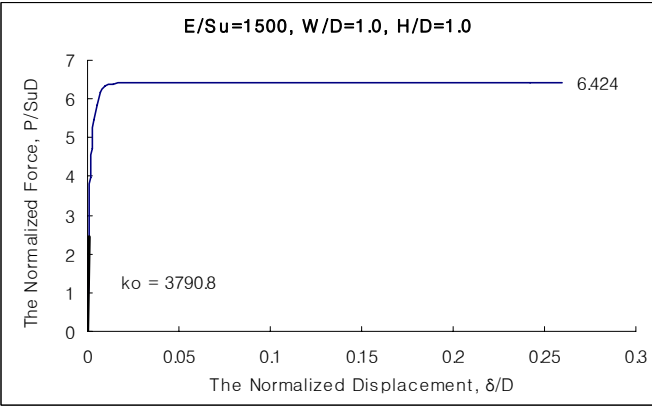
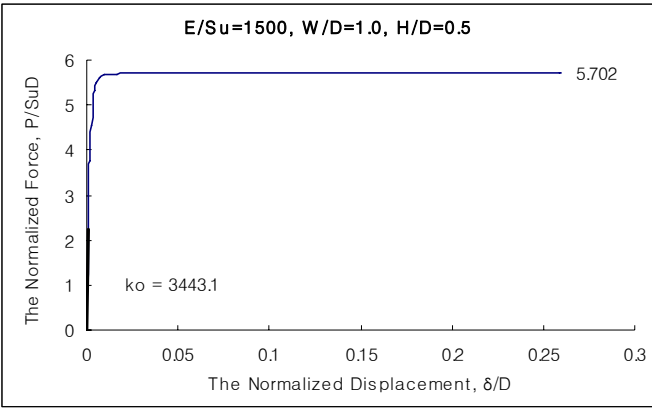


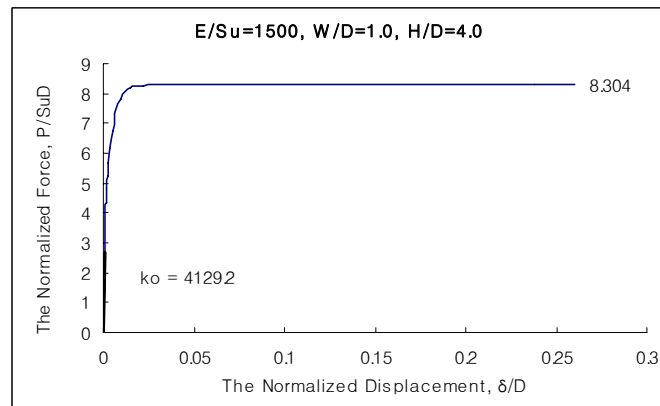
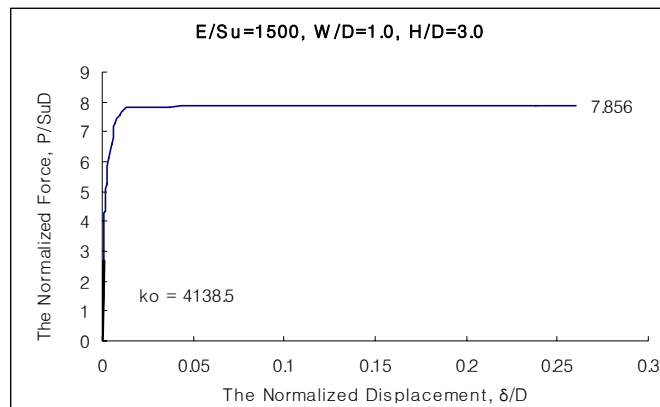












APPENDIX B**A TYPICAL ABAQUS INPUT FILE: NONLINEAR SOIL SPRING MODEL**

```

*HEADING
  W/D=1.0, H/D=1.0, Es/Su=100 (unit : lb, in)
*PRE PRINT, ECHO=NO, MODEL=NO, CONTACT=NO, HISTORY=NO
*PARAMETER
  L=3600
  ele=200
  n=ele+1
  Ep=3e7
  D=6
  r=D/2
  t=0.5
  u=1
  su=1
  Pmax=6.4*su*D*dx
  dy=0.0235*D
*NODE
  1,0,-3
  <n>,<L>,-3
*NGEN
  1,<n>
*NSET, NSET=PIPENODE
  1,<n>
*ELEMENT, TYPE=PIPE21
  1,1,2
*ELGEN, ELSET=PIPE
  1,<ele>
*BEAM SECTION, SECTION=PIPE, ELSET=PIPE, MATERIAL=STEEL
  <r>, <t>
*MATERIAL, NAME=STEEL
*ELASTIC
  <Ep>
*ELEMENT, TYPE=SPRING1
  10001,1
*ELGEN, ELSET=SOILSPRING
  10001,<ele>
*SPRING, ELSET=SOILSPRING, NONLINEAR
  2
  --<Pmax>, --<dy>
     0, 0
     <Pmax>, <dy>
*****
*STEP, INC=1000, NLGEOM
*STATIC
*BOUNDARY
  <n>,2,2
*BOUNDARY, TYPE=DISPLACEMENT
  1,2,2,<u>
*OUTPUT, FIELD, FREQ=100
*ELEMENT OUTPUT, ELSET=PIPE
  COORD, S
*EL PRINT, ELSET=PIPE
  COORD
  S11
*END STEP

```


APPENDIX C**MATLAB PROGRAM: LINEAR SOIL SPRING MODEL**

```

clc
clear all

%===== Input Variables =====%

L=3600;           % Length of touchdown zone (pipe length)
ele=1000;         % Number of elements
dx=L/ele;        % Unit length of pipe

E=3e7;           % Modulus of pipe
D=6;             % Diameter of pipe
t=0.5;          % Thickness of pipe

u=1;             % Displacement

Su=1;            % Undrained shear strength
kn=272;          % Normalized spring constant
ko=kn*Su;        % Spring constant [F/L^2]

%==== Basic Calculation ====%

c=0.5*D-t/2;     % Distance from center to end of pipe
I=pi/64*(D^4-(D-2*t)^4); % Second moment inertia

%===== Initialize =====%

K=zeros(ele-1,ele-1);
p=zeros(ele-1,1);

%===== Main Loop =====%

for i=3:(ele-3)
    for j=1:(ele-1)
        if j==i-2
            K(i,j)=1;
        elseif j==i-1
            K(i,j)=-4;
        elseif j==i
            K(i,j)=6+ko*dx^4/(E*I);
        elseif j==i+1
            K(i,j)=-4;
        elseif j==i+2
            K(i,j)=1;
        end
    end
end

p(1,1)=2*u; p(2,1)=-u;
K(1,1:5)=[(5+ko*dx^4/(E*I)) -4 1 0 0];

```

```

K(2,1:5)=[-4 (6+ko*dx^4/(E*I)) -4 1 0];
K(ele-2,ele-5:ele-1)=[0 1 -4 (6+ko*dx^4/(E*I)) -4];
K(ele-1,ele-5:ele-1)=[0 0 1 -4 (5+ko*dx^4/(E*I))];
yy=inv(K)*p;

y(1,1)=u;
y(2:ele,1)=yy;
y(ele+1,1)=0;

%===== Moment Calculation =====%

for i=2:ele
    ddy(i,1)=(y(i-1,1)-2*y(i,1)+y(i+1,1))/dx^2;
    M(i,1)=-E*I*ddy(i,1);
    Bsigma(i,1)=M(i,1)*-c/I;
end

%===== Plot =====%

xNODE(1)=0; xELE(1)=0;
for j=2:(ele+1)
    xNODE(j)=xNODE(j-1)+dx;
end
for j=2:ele
    xELE(j)=xELE(j-1)+dx;
end

figure(1)
plot (xNODE,y, 'b-', 'LineWidth', 2)
axis auto
title('The Deflection along the pipe
length', 'fontsize', 12, 'fontweight', 'bold')
xlabel('The Length along the pipe', 'fontsize', 10, 'fontweight', 'bold')
ylabel('The Deflection', 'fontsize', 10, 'fontweight', 'bold')

figure(2)
plot (xELE,Bsigma, 'b-', 'LineWidth', 2)
axis auto
title('The Bending Stress along the pipe
length', 'fontsize', 12, 'fontweight', 'bold')
xlabel('The Length along the pipe', 'fontsize', 10, 'fontweight', 'bold')
ylabel('The Bending Stress', 'fontsize', 10, 'fontweight', 'bold')

```

APPENDIX D**MATLAB PROGRAM: NONLINEAR SOIL SPRING MODEL**

```

clc
clear all

%===== Input Variables =====%

L=3600;           % Length of touchdown zone (pipe length)
ele=1000;        % Number of elements
dx=L/ele;        % Unit length of pipe

E=3e7;           % Modulus of pipe
D=6;             % Diameter of pipe
t=0.5;          % Thickness of pipe

u=1;             % Displacement

Su=1;            % Undrained shear strength
Pn=6.40;         % Normalized maximum force
kn=272;          % Normalized spring constant

Pmax=Pn*Su*D;    % Maximum force [F/L]
ko=kn*Su;        % Spring constant [F/L^2]
deltay=Pmax/ko;  % Deformation [L]

%==== Basic Calculation ====%

c=0.5*D-t/2;     % Distance from center to end of pipe
I=pi/64*(D^4-(D-2*t)^4); % Second moment inertia;

%===== Initialize =====%
z=100;
a=1;
count=1;
K=zeros(ele-1,ele-1);
p=zeros(ele-1,1);
yy=zeros(ele-1,1);
by=zeros(ele-1,z);

%===== MAIN LOOP =====%

while ( a~=0 )

    K=zeros(ele-1,ele-1);
    p=zeros(ele-1,1);
    k=zeros(ele-1,1);

    if count>1
        for m=1:(ele-1)

```

```

        by(m,count-1)=yy(m,1);
        if yy(m,1)>deltay
            k(m,1)=Pmax/yy(m,1);
        elseif yy(m,1)<=-deltay
            k(m,1)=-Pmax/yy(m,1);
        else
            k(m,1)=ko;
        end
    end
else
    for m=1:(ele-1)
        k(m,1)=ko;
    end
end

%=== decide k(spring constant) ===%
yy=zeros(ele-1,1);
for i=3:(ele-3)
    for j=1:(ele-1)
        if j==i-2
            K(i,j)=1;
        elseif j==i-1
            K(i,j)=-4;
        elseif j==i
            K(i,j)=6+k(i,1)*dx^4/(E*I);
        elseif j==i+1
            K(i,j)=-4;
        elseif j==i+2
            K(i,j)=1;
        end
    end
end

p(1,1)=2*u; p(2,1)=-u;
K(1,1:5)=[(5+k(1,1)*dx^4/(E*I)) -4 1 0 0];
K(2,1:5)=[-4 (6+k(2,1)*dx^4/(E*I)) -4 1 0];
K(ele-2,ele-5:ele-1)=[0 1 -4 (6+k(ele-2,1)*dx^4/(E*I)) -4];
K(ele-1,ele-5:ele-1)=[0 0 1 -4 (5+k(ele-1,1)*dx^4/(E*I))];
end

yy=inv(K)*p;

if count>1
    a=0;
end

for n=1:(ele-1)
    if count>1
        ij(n,count)=abs(yy(n,1)-by(n,count-1))/abs(by(n,count-1));
        if ij(n,count)>0.01
            a=a+1;
        end
    end
end
end

```

```

        count=count+1;

end

y(1,1)=u;
y(2:ele,1)=yy;
y(ele+1,1)=0;

%===== Moment Calculation =====%
for i=2:ele
    ddy(i,1)=(y(i-1,1)-2*y(i,1)+y(i+1,1))/dx^2;
    M(i,1)=-E*I*ddy(i,1);
    Bsigma(i,1)=M(i,1)*-c/I;
end

%===== plot =====%
xNODE(1)=0; xELE(1)=0;
for j=2:(ele+1)
    xNODE(j)=xNODE(j-1)+dx;
end
for j=2:ele
    xELE(j)=xELE(j-1)+dx;
end

figure(1)
plot (xNODE,y,'b-','LineWidth',2)
axis auto
title('The Deflection along the pipe
length','fontsize',12,'fontweight','bold')
xlabel('The Length along the pipe','fontsize',10,'fontweight','bold')
ylabel('The Deflection','fontsize',10,'fontweight','bold')

figure(2)
plot (xELE,Bsigma,'b-','LineWidth',2)
axis auto
title('The Bending Stress along the pipe
length','fontsize',12,'fontweight','bold')
xlabel('The Length along the pipe','fontsize',10,'fontweight','bold')
ylabel('The Bending Stress','fontsize',10,'fontweight','bold')

```

APPENDIX E**MATLAB PROGRAM: TENSION CUT-OFF SOIL SPRING MODEL**


```

clc
clear all

%===== Input Variables =====%

L=3600;           % Length of touchdown zone (pipe length)
ele=1000;        % Number of elements
dx=L/ele;        % Unit length of pipe

E=3e7;           % Modulus of pipe
D=6;             % Diameter of pipe
t=0.5;          % Thickness of pipe

u=1;             % Displacement

Su=1;            % Undrained shear strength
Pn=6.40;        % Normalized maximum force
kn=272;         % Normalized spring constant

Pmax=Pn*Su*D;   % Maximum force [F/L]
ko=kn*Su;       % Spring constant [F/L^2]
deltay=Pmax/ko; % Deformation [L]
ratio=0.5;      % ratio of Pmax in tension to Pmax in compression

%===== Basic Calculation =====%

c=0.5*D-t/2;    % Distance from center to end of pipe
I=pi/64*(D^4-(D-2*t)^4); % Second moment inertia

%===== Initialize =====%
z=100;
a=1;
count=1;
K=zeros(ele-1,ele-1);
p=zeros(ele-1,1);
yy=zeros(ele-1,1);
by=zeros(ele-1,z);

%===== MAIN LOOP =====%

while ( a~=0 )

    K=zeros(ele-1,ele-1);
    p=zeros(ele-1,1);
    k=zeros(ele-1,1);

    if count>1
        for m=1:(ele-1)
            by(m,count-1)=yy(m,1);
        end
    end

```

```

        if yy(m,1)>deltay*ratio
            k(m,1)=0;
        elseif yy(m,1)< -deltay
            k(m,1)=-Pmax/yy(m,1);
        else
            k(m,1)=ko;
        end
    end
else
    for m=1:(ele-1)
        k(m,1)=ko;
    end
end

%=== decide k(spring constant) ===%
yy=zeros(ele-1,1);
for i=3:(ele-3)
    for j=1:(ele-1)
        if j==i-2
            K(i,j)=1;
        elseif j==i-1
            K(i,j)=-4;
        elseif j==i
            K(i,j)=6+k(i,1)*dx^4/(E*I);
        elseif j==i+1
            K(i,j)=-4;
        elseif j==i+2
            K(i,j)=1;
        end
    end
end

p(1,1)=2*u; p(2,1)=-u;
K(1,1:5)=[(5+k(1,1)*dx^4/(E*I)) -4 1 0 0];
K(2,1:5)=[-4 (6+k(2,1)*dx^4/(E*I)) -4 1 0];
K(ele-2,ele-5:ele-1)=[0 1 -4 (6+k(ele-2,1)*dx^4/(E*I)) -4];
K(ele-1,ele-5:ele-1)=[0 0 1 -4 (5+k(ele-1,1)*dx^4/(E*I))];
end

yy=inv(K)*p;

if count>1
    a=0;
end

for n=1:(ele-1)
    if count>1
        ij(n,count)=abs(yy(n,1)-by(n,count-1))/abs(by(n,count-1));
        if ij(n,count)>0.01
            a=a+1;
        end
    end
end
count=count+1;

```

```

end

y(1,1)=u;
y(2:ele,1)=yy;
y(ele+1,1)=0;

%===== Moment Calculation =====%
for i=2:ele
    ddy(i,1)=(y(i-1,1)-2*y(i,1)+y(i+1,1))/dx^2;
    M(i,1)=-E*I*ddy(i,1);
    Bsigma(i,1)=M(i,1)*-c/I;
end

%===== plot =====%
xNODE(1)=0; xELE(1)=0;
for j=2:(ele+1)
    xNODE(j)=xNODE(j-1)+dx;
end
for j=2:ele
    xELE(j)=xELE(j-1)+dx;
end

figure(1)
plot (xNODE,y,'b-','LineWidth',2)
axis auto
title('The Deflection along the pipe
length','fontsize',12,'fontweight','bold')
xlabel('The Length along the pipe','fontsize',10,'fontweight','bold')
ylabel('The Deflection','fontsize',10,'fontweight','bold')

figure(2)
plot (xELE,Bsigma,'b-','LineWidth',2)
axis auto
title('The Bending Stress along the pipe
length','fontsize',12,'fontweight','bold')
xlabel('The Length along the pipe','fontsize',10,'fontweight','bold')
ylabel('The Bending Stress','fontsize',10,'fontweight','bold')

```

VITA

Jung Hwan You was born on November 2, 1976 in Seoul, Korea. During 1996-1998, he served his country in the Defense Security Command (DSC) of the Republic of Korea Army. He received his Bachelor of Science degree in civil engineering from Yeungnam University in February 2002. In the fall of 2003, he enrolled in the Department of Civil Engineering at Texas A&M University in order to pursue the M.S. degree. He received his M.S. degree in December 2005.

His permanent address is:

Samsung apt. 106-1301

Dalseo-gu Hosan-dong

Daegu 704-741, S.Korea.